TECHNICAL MEMORANDUM

92

The 1984 revision of the ECMWF analysis system

D. Shaw, P. Lönnberg and
A. Hollingsworth

Research Department

October 1984

European Centre for Medium-Range Weather Forecasts
Europäisches Zentrum für mittelfristige Wettervorhersage
Centre européen pour les prévisions météorologiques à moyen

Abstract

A comprehensive evaluation of the ECMWF operational data assimilation system has been made, based largely on statistics of its performance over a long period of time. The evaluation has identified many deficiencies, covering such aspects of the analysis as the optimum interpolation statistics, the data selection algorithms, and the quality control criteria applied within the analysis.

The observation and forecast error variances were seriously in error in the stratosphere and in the tropics. A more faithful model of the forecast error spectrum is provided by the Bessel function expansion than by the Gaussian model. The vertical structure of the height error is assumed to be composed of two components: a 'barotropic' part related to a horizontally constant mode and a 'baroclinic' structure for the horizontally varying models. The extratropical vertical correlation remained similar to the earlier correlations, but the tropical height and wind structures changed dramatically.

Reasonable rejection limits were defined from the distributions of the observation departures from the first-guess, as were observation errors for satellite and aircraft wind reports and Australian pseudo-observations.

A comprehensive and homogeneous data selection algorithm has been devised. This has entailed amendments to the data thinning algorithm, the priorities given to different types of data, the positions of the slab boundaries in the vertical, the algorithms to ensure a representative selection of data, and many other minor changes.

The results of the improvement, in a series of tests, covering in total some 30 days of assimilations, are also described. In summary they yield an analysis and a subsequent first-guess which are in closer agreement with observations. The analysis scheme yields more balanced fields in the sense that the subsequent initialisation produces more modest changes. The major impact on forecasts, in particular short range, is also judged to be positive.

C O N T E N T S

		PAGE
1.	INTRODUCTION	2
2.	THE DATA SELECTION AND DATA USAGE	3
2.1	Superobbing formation	6
2.2	Designation of observations as secondary	7
2.3	Slab boundaries	8
2.4	Box selection	9
2.5	Forcing radius	9
2.6	Subregion division of the analysis boxes	9
2.7	Other minor changes	10
2.8	An example	12
2.9	Problems in preprocessing data	14
3.	THE OI STATISTICS	20
3.1	Horizontal correlations	20
3.2	Vertical correlations	25
3.3	Accuracy of the first guess field	27
3.4	Observation error statistics	28
4.	QUALITY CONTROL CHECKS	31
5.	THE ANALYSIS OF UPPER LEVEL GEOPOTENTIALS	38
6.	THE IMPACT OF ANALYSES ON THE CHANGES	40
6.1	Quality control	41
6.2	Fit to the observations	50
6.3	The relative roles of F, A, I	51
6.4	The quality of the forecasts	57
7.	CONCLUSIONS	63

1. INTRODUCTION

The global data assimilation scheme at ECMWF has been used operationally since late 1979. In the first three years of operational working many revisions were made to the assimilation technique, based partly on operational experience and partly on experience gained from the FGGE analyses, which the Centre produced using the same technique. The individual revisions were introduced operationally as they became available, and no doubt contributed to the gradual improvement in the quality of the Centres forecasts which is discernible from various studies.

By the end of 1982 this first phase of development was coming to an end. Obvious deficiencies which were easily rectified had been removed. Weaknesses were still evident in the system, but some were recognised as requiring more extensive evaluation than was possible by the examination of brief sequences of case studies. Comprehensive statistics were required to evaluate the assimilation technique. To this end a diagnostics package was incorporated (with effect from late 1982) in the operational suite whereby the performance of the assimilation system, measured against the observational datum presented to it, is recorded and archived. Quantities recorded are the departure of the observational data from the first guess value, from the analysed value, and from the initialised value. As data are considered for use within the analysis, they undergo various quality control checks; all quality control events associated with each datum are also recorded in this 'assimilation statistics' package. The analysis is, in fact, an analysis of departures from the first guess, and so it is appropriate to record the first guess, analysed and initialised departures from the observational data, at the observation locations.

Assimilation statistics of the type described are extremely valuable, with several possible applications. One such application is the identification of possible data errors at particular observing platforms, as described by ECMWF Staff Members (1984). Another is the re-evaluation of the statistical properties ascribed in the optimum interpolation (OI) technique used in the analysis, which is partly covered in this paper but pursued fully in

Hollingsworth and Lönnberg ,1984. Two further benefits of the statistics are that they provide a means of assessing the efficacy of the quality control algorithms of the analysis, and that they permit the usage of data within the analysis to be comprehensively monitored.

It became evident from an investigation of these and other aspects of the analysis that substantial improvements could be made within the framework of the existing analysis programs, and to this end a comprehensive package of changes have been produced and extensively tested. The purpose of this paper is to describe these changes, and to evaluate their impact on the assimilations and ensuing forecasts. The changes fall into four basic categories:

- a revision of the data selection and data usage

- a revision of the OI statistics

- a revision of the quality control criteria

- a revision of the method of analysing geopotential height in the upper levels of the analysis

The next four sections of the paper describe these changes in turn. The later sections describe the impact of the changes as seen in benchmark experiments carried out prior to operational implementation, which occurred in May 1984.

2. THE DATA SELECTION AND DATA USAGE

The data selection algorithms of the analysis are very complicated. The ECMWF Data Assimilation Scientific Documentation (Lönnberg and Shaw,1983) describes in appropriate detail the working of the selection process. It omits some of the finer details, and certainly many of the practical ramifications of the algorithms are only appreciated by study of practical examples.

One of the considered strengths of the analysis technique is the concept of making the selection comprehensive - i.e. it seeks to select a substantial body of data (up to 191, the current maximum matrix dimension) in the calculations for a particular analysis volume. The computational expense of such a selection is offset by using the same selection for all grid points lying within the analysis volume. These analysis 'boxes' have horizontal dimensions of approximately 660x660 kms and their locations remain unchanged with successive analyses. In the vertical there is the facility of splitting the full depth of the 15 analysis levels into three slabs when the need arises (i.e. when the data is more than moderately dense). Prior to the changes the vertical division of these slabs was 1000-700, 500-150, and 100-10 mbs. In making the selection of data for the analysis of grid points within a particular box it is desirable to include data both from inside and from outside the box, to ensure a representative sampling, particularly for the analysis of grid points near the boundaries. In a data dense region there may well be a choice of several hundred data from which to make a selection. A representative sampling is required, and an important aid to this end is the process of 'super-obbing' - condensing consistent and closely adjacent observations into a single observation (a 'superob'). Following this consideration, some appropriate selection is still required. This is done in stages, selecting first the analysis boxes from which data will be selected; then selecting observations from within these boxes; and finally selecting data from within these observations. At each stage constraints are applied with the intention of excluding immoderate volumes of data.

The practical performance of the data selection algorithm in data dense regions fell far short of expectations. The extent of the problem can be seen in Fig. 1, which shows the selection of observations made for an analysis box (lowest slab) in the data rich European area for a 12 GMT analysis, the date being chosen at random. Three deficiencies are seen. Firstly there are data gaps within the central box - not all the observations within the box are selected. Secondly very few observations are selected

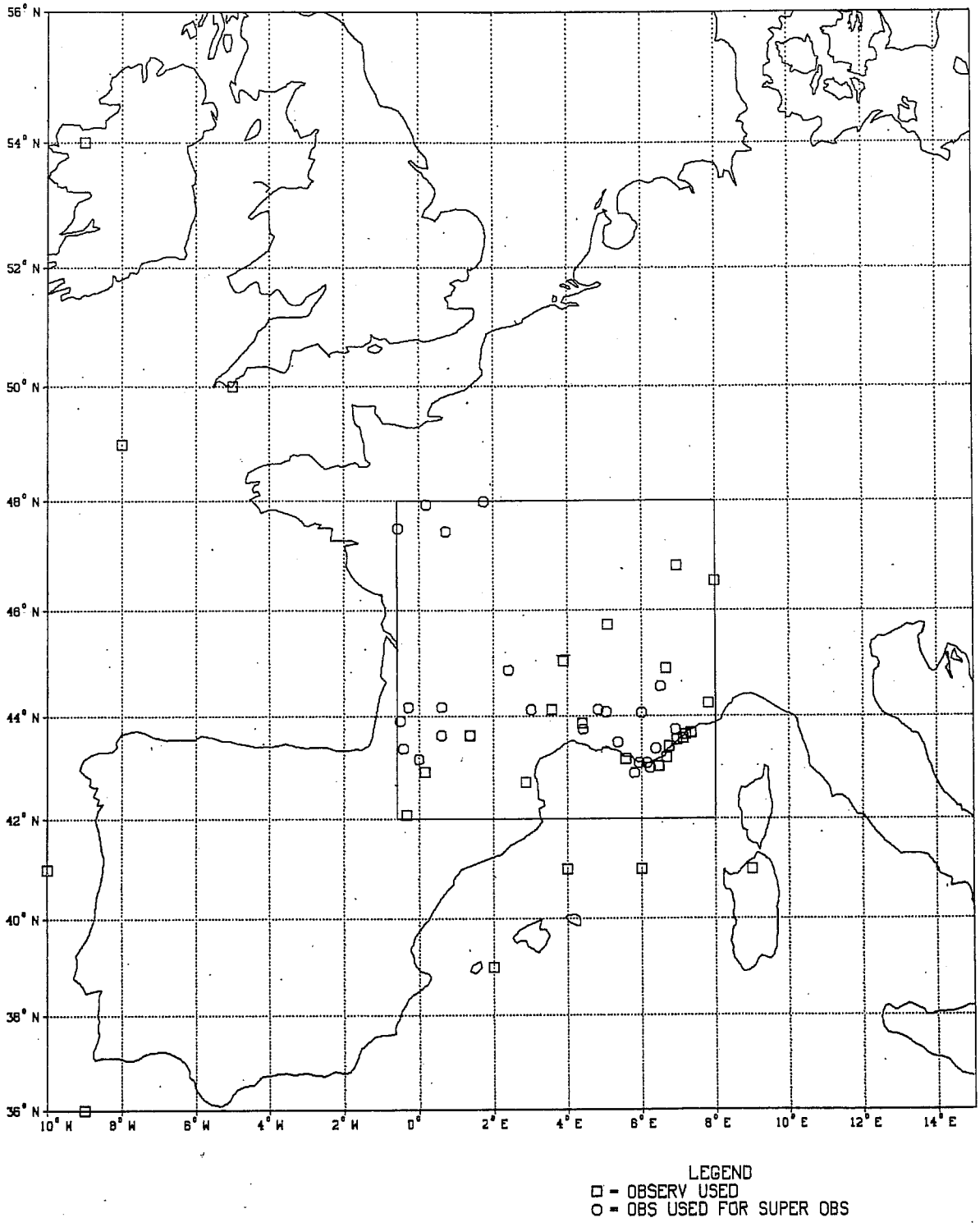

Fig. 1 Observations selected for the analysis of the rectangular box shown, using the original data selection algorithm. 12 GMT 7.5.83.

from outside the central box. Indeed the only such observations selected happen to be satellite thickness data, some of which are from inappropriately distant locations. Thirdly there is a dense cluster of observations (mainly SYNOPS) along the south coast of France which should have been superobbed into a fewer number of observations but which have been preserved as separate items of data, leading to a rapid filling of the matrix.

The causes of this unsatisfactory selection of observations are numerous, ranging from weaknesses in the algorithm itself to deficiences in the coding of the algorithm. Investigation led to the following set of revisions, the objective being to seek a comprehensive and representative sampling of the observations.

2.1 Superobbing formation

The superobbing algorithm is described in detail in Lönnberg and Shaw (1983). There are two major practical weaknesses in the formation of such observations. For data pairs which are superobbing candidates approximately 45% fail to be superobbed because of the stringency of two distinct compatibility requirements. The first such requirement is that the two data should be mutually compatible. This is expressed as

$$(\delta^o_i - \delta^o_j)^2 \leq \text{BUDTOL}\ (\varepsilon^{o2}_i + \varepsilon^{o2}_j)$$

Here δ^o_i, δ^o_j are the departures of the observations at i,j from their respective first guess values normalised by the first guess error, and ε^o_i , ε^o_j are ascribed rms observation errors normalised by the first guess error. In the original formulation BUDTOL=1.

For a SYNOP pressure, with an ascribed rms error of 1 mb, this requires the difference between the two data to be less than 1.4 mb. A more reasonable value of BUDTOL is 2, which relaxes the requirement to 2 mb. The second compatibility requirement is that each datum should be close to the first guess. This is expressed as

$$\delta^{o2}_i \leq \text{BUDDEV}\ (1 + \varepsilon^{o2}_i)$$

In the original formulation BUDDEV=2.25

For a SYNOP pressure over Europe, and using a value of first guess rms error of 1.3 mb(a value suggested by revised estimates of the first guess error) the departure limit is 2.2 mb. It only requires a modestly poor first guess and no superobbing will occur. BUDDEV has now been increased to 9, relaxing the requirement from 2.2 to 4.4 mb.

The effect of relaxing these two requirements is that in tests the superob failure rate drops from 45% to 25%, and so the volumes of surface data passed to the later stages of the analysis are much more modest and manageable. An indication that too much superobbing is now permitted would be rejection of superobs in the final data checking stage; such occurrences are very rare. The failure rate of 25% is perhaps still rather high, bearing in mind that only approximately 1% of SYNOPS are finally judged to be wrong, but it should be remembered that a proportion of the failures are where a poor first guess prevents superobbing, and in such situations preservation of the separate observations is desirable to provide mutual support in the subsequent data checking step. Further tuning of the tolerances is possible but it is felt that a reasonable balance has now been struck.

2.2 Designation of observations as secondary

In the original system an observation (or superob) was designated as either 'primary' or 'secondary'. An observation within approximately 190 kms of another more important observation (this judgment being based on observation type) is deemed to be secondary, while the more important one becomes primary. Secondary observations receive less consideration in subsequent selection judgments, and it has been found that this system produces unsatisfactory results. In tests, examples were found of observations migrating 100 kms to form a superob; this superob was then rendered secondary by another observation perhaps 190 kms away, effectively denuding the original data network on scales of 300 kms. The other weakness of secondary observation discrimination is the different treatments of such data later in

the selection process. Complete boxes of secondary observations can be lost at the box selection stage if they are non-central; if however the secondary observation survives beyond the box selection stage then the fact that it is secondary becomes irrelevant. Both features were found to have unsatisfactory consequences in the original system.

The concept of secondary observations has been almost abandoned. Such designation is now avoided in the buddy-checking/superobbing procedures. The only stage at which a secondary observation can now be formed in the new system is when a surplus of primary observations are left in a box at the end of the analysis preprocessing (i.e. after the superobbing etc); if at this stage the number of observations exceeds a permitted limit (40) then the surplus observations are made secondary. In tests carried out on a 12 GMT analysis this limit was never met, the maximum number of observations in a box having been condensed to only 34, all of which are classed as primary.

2.3 Slab boundaries

The vertical slab boundaries have been adjusted, changing the upper limit of the bottom slab from 700 to 850 mb. Thus where a three slab analysis is being done the bottom slab selection will take data from its own levels of 1000 mb and 850 mb, together with one overlap level, namely 700 mbs. This produces a generally more equitable availability of data for the bottom two slabs of the atmosphere; in particular it allows considerably more surface data to be used in the bottom slab. In a sample box in a data rich region the selection of data for the bottom slab at 12 GMT, using the fully revised selection algorithm, was:

	1000	850	700
h	58	28	12
v	14	18	13
Δh	0	2	1

This indicates a reasonable mix of geopotential and wind data, bearing in mind that each wind has two components associated with it. The selection of (SATEM) thickness data is limited because the area in question happened to be mainly over land, where such data are currently excluded.

2.4 Box selection

In the selection of boxes, the central box and its immediate neighbours are guaranteed selection. However in the old system there was no guarantee that boxes close to, but not touching, the central box were selected. Thus observations almost touching the central box could be lost at the box selection stage, where it was judged that a sufficiency of data had already been assured from other boxes. This was occurring over the European region and probably other regions as well. The new algorithm guarantees not only selection of immediately adjacent boxes but their immediate neighbours too. As a further precaution against premature exclusion of observations at the box selection stage, the data limits described by Lönnberg and Shaw(1983) have been removed.

2.5 Forcing radius

In the selection of observations, all observations within a certain distance of the centre of the central box are forced into the selection (though this does not guarantee their selection at the subsequent data selection stage). This forcing radius is 660 kms in the operational system- insufficient if one is seeking to include a reasonable overlap of data and possibly does not include an observation within 200 km of a grid point. It has therefore been increased to $\sqrt{2}.660$ kms which is sufficiently large to embrace all observations in the subregions discussed below.

2.6 Subregion division of the analysis boxes

Having selected the boxes from which observations are to be selected, and having forced in observations within the forcing radius, the process of selection continues with a reordering of all observations by distance from the centre of the central box. The purpose of this is to give preference to the very central observations. Unfortunately in so doing there is a probability that the matrix is filled with data concentrated near this

central point, with no data being drawn from the extremities of the box or beyond. In the new system this is avoided by a further partial reordering of the observations which ensures a more representative sampling. The analysis box (with dimensions of approximately 660x660 kms) and the outlying regions, defined by a half-box extension of the central box are divided into 16 subregions, each of approximately dimension 330x330 kms, as shown in Fig. 2. These 16 subregions represent the overall area from which data should be drawn to provide a reasonable analysis for the central box in a data rich region (elsewhere, where there is a paucity of data, more distant sampling of data should and does occur). It remains to make the selection representative. For a matrix size of 191 the 16 subregions can be permitted to contribute approx 12 data each (not very many for such large subregions). To this end the observations are reordered, drawing observations from the subregions in the sequence indicated in the numbering of Fig. 2. In this process preference is given to particular types of observation, the order being TEMP, PILOT, SATEM, SYNOP/SHIP, AIREP, SATOB and DRIBU. Each observation is deemed to contribute a fixed number of data to the matrix. In practice this will not be the case and will depend not only on the individual observation but also on the slab being analysed. However overall values are set, namely 9, 6, 2, 3, 2, 2 and 1 for the above observation types, respectively. Thus having selected two TEMPS from a particular subregion, the selection would proceed to the next subregion. When the subregions have been sampled sufficiently to exceed the matrix size (using this fixed volume assumption for each observation type), or when all 16 subregions have been considered, the selection by subregion stops and all remaining observations are sequenced (retaining their distance-from-centre order) to follow the newly selected observations. This leaves the observations in an order which should ensure that the final data selection will be representative, giving preference to such observations as TEMPS. It does not guarantee the use of all available observations, which is not possible given the overall size of the analysis area and the current limits of the matrix size.

2.7 Other minor changes

As well as the major changes described above, other minor changes were made to the selection coding, and and these are included here for completeness

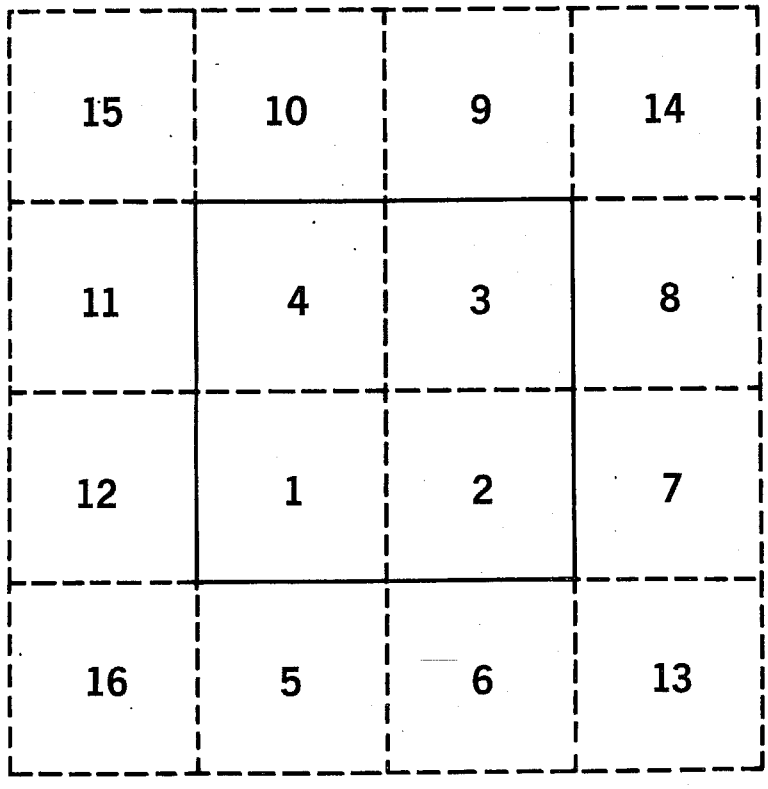

Fig. 2 Subregion division of analysis boxes, used in the new selection algorithm. The full line marks box boundaries, the dashed lines mark subregion boundaries. The numbers indicate the sequence in which the subregions are sampled.

since they do have a bearing on the final selection.

(a) In the selection of observations a limit is imposed on the total that can be selected. The value of 100 quoted in Lönnberg and Shaw (1983) was found to be insufficient; one box may have as many as 34 observations and so there is little scope for drawing data from outside the first few boxes considered. This number has been increased to 200, which is sufficient to avoid imposing an unnecessary constraint on the selection at this stage.

(b) When working in the three slab mode, the selection for a particular slab was restricted to data within the slab, save for the selection of supplementary data if there is a lack of sufficient data within the slab. This can produce discontinuities across slab boundaries and to reduce this possibility the selection for each slab now embraces the immediately adjacent levels outside the slab.

(c) The maximum number of primary observations permitted in a box at the end of the pre-processing is set to 40, as already mentioned; previously this maximum was 90. The information in question is written out to a workfile with control information preceeding the meteorological data, with practical limits imposed on the buffer lengths. The penalty of having an unreasonably high upper limit is that the major part of the record will be filled with control information at the expense of the meteorological data.

(d) It was found in practice that the matrix dimension finally used fell considerably short of the maximum of 191, even in data rich regions. Only data checked in the data checking step of the analysis is permitted to enter the final analysis. Data that have not been checked are excluded and in finding such a circumstance the original code was reducing the matrix dimension by one for each datum so found, rather than selecting another datum. Consequently the final matrix dimension could easily be reduced by perhaps 30 or more. This reduction is now avoided.

2.8 An example

The benefits of the above set of revisions can be judged from Fig. 3, which shows, for the same case as Fig. 1, how the selection of data is changed. Firstly, all appropriate data originally selected have been retained. Indeed in this particular case every single datum available within the central box has been selected (such a complete selection cannot be guaranteed in all

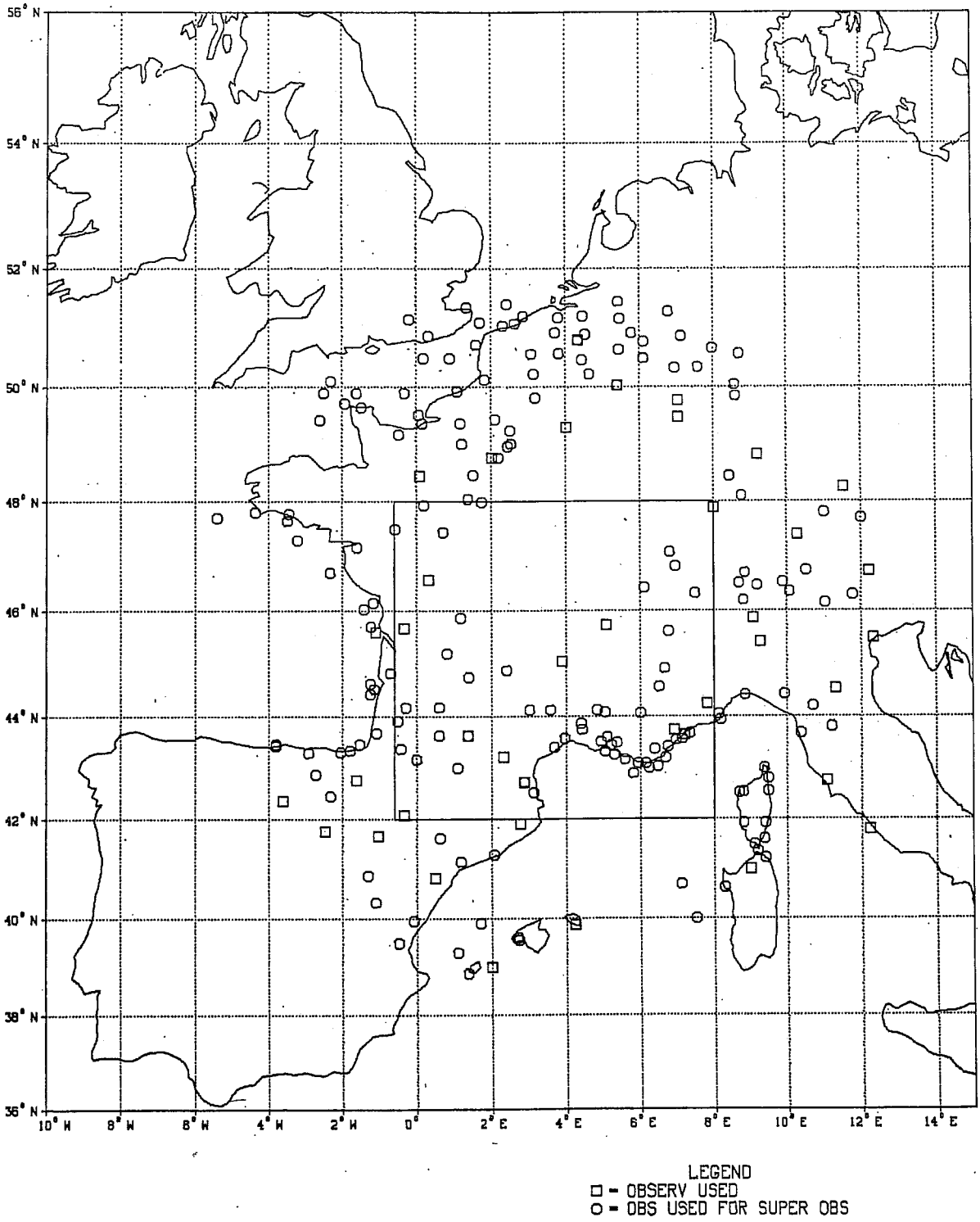

Fig. 3 As Fig. 1, using the new data selection algorithm.

other cases). Secondly the selection of data now extends beyond the boundaries of the central box, giving a good sampling of data out to approximately 300 kms outside the box, and excluding the irrelevant and very distant data of the original selection. Thirdly an effective superobbing of closely adjacent and compatible observations now occurs. There is an apparent data void region in eastern France, where one would expect to see SYNOP observations. This void is a consequence of the 'envelope' orography of the prediction model- SYNOP data cannot be used because of the excessive extrapolation required of the first guess field. Data so discarded are not shown in Figs. 1 and 3.

The practical benefits of the improved data selection algorithm are discussed later. The remaining deficiencies are not easily removed within the structure of the existing code. The two serious weaknesses remaining are the excessive complexity of the scheme, and the inability to guarantee the selection of observations which may in certain circumstances prove critical. These features can only be addressed in a total revision of the selection scheme which is beyond the scope of this present study.

2.9 Problems in preprocessing data

The above account relates to the selection of data considered for use in the analysis. It presupposes that data chosen will not usually be detrimental to the analysis. This may not be the case if observational information is incorrectly preprocessed or if particular types of data are used which cannot be correctly exploited by the system. The assimilation statistics permit the computation of time averaged (observed - first guess) values at a reporting platform for a selected period. In this way systematic biases of either the observed or the first guess may be detected. Such a study has revealed two serious weaknesses in the operational system, both relating to the use of near-surface information; while the symptoms are similar the causes of the two problems are distinct.

An important observed parameter which the original analysis system sought to use is surface wind, from both SHIPS and land SYNOPS (provided the latter has a station height below 500 m). Such a parameter is expressed as a departure from a first guess 10 m wind, which is not available directly from the

prediction model but which is diagnosed by extrapolation from the lowest model level wind (see ECMWF Forecast Model Scientific Documentation, Louis, 1983). Statistics have been produced of (observed - first guess) 12 GMT 10 m winds for frequently reporting land SYNOPS for January 1983, see Fig. 4. It reveals large systematic differences, typically 3-7 m/s over substantial regions. The fact that the biases are regional suggests that the problem lies with the first-guess wind rather than with the observational data. The difference is against the prevailing wind - the obvious interpretation being that the first guess wind is too strong. This is substantiated by the realisation that the use of such data , coupled with the use of surface pressure data,yields pressure and wind analysis increments which tend to lack the full amount of geostrophic balance which we would expect. In the analysis of a feature such as a depression, the use of land SYNOP winds induce analysed wind increments counter to the prevailing wind, hence reducing the circulation round the analysed feature and, through geostrophic coupling, relaxing the pressure gradients and so filling the depression. The process of extrapolation of the model structure to provide a first guess 10 m wind is very dependent on the geographically dependent, ascribed roughness length (see Louis, 1983) and one is led to the conclusion that the roughness lengths assumed ,in some regions at least, are inappropriate. A global map of the type of bias shown in Fig 4 allows the problem to be inverted - such a map could be used to redefine the roughness length so as to eliminate the regional differences of observed and first guess states; this is currently being considered. The discrepancies are most serious in coastal regions; at fixed oceanic platforms in open sea (e.g. the ocean weather ships) no appreciable bias has been detected, suggesting that SHIP wind data can usefully be exploited in the analyses. In the new system land SYNOP winds are now discarded. Exclusion of such data permits, as an example, the number of SYNOP pressure values selected in the analysis to be tripled. The impact of the change can be seen in Fig. 5(a) and (b), which shows two analyses of (initialised) mean sea level pressure, first with, and then excluding, land SYNOP winds. The occasion, chosen at random, shows a general north/south gradient of surface pressure over southern Europe. Data coverage is sufficient to define the true pressure field with confidence. A difference is

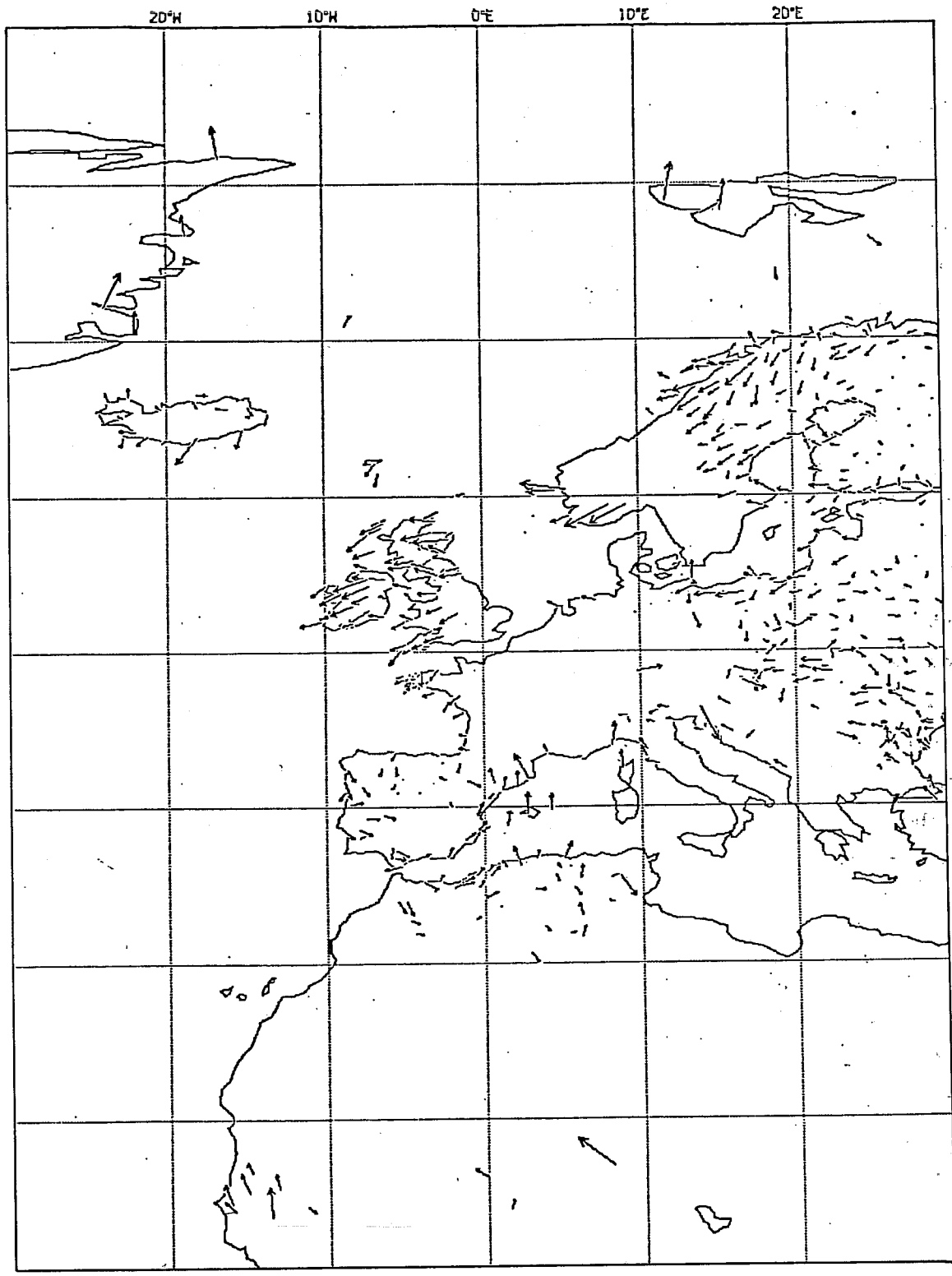

Fig. 4 Biases (observed-first guess) 10 m winds, based on 12 GMT data for Jan. 1983.

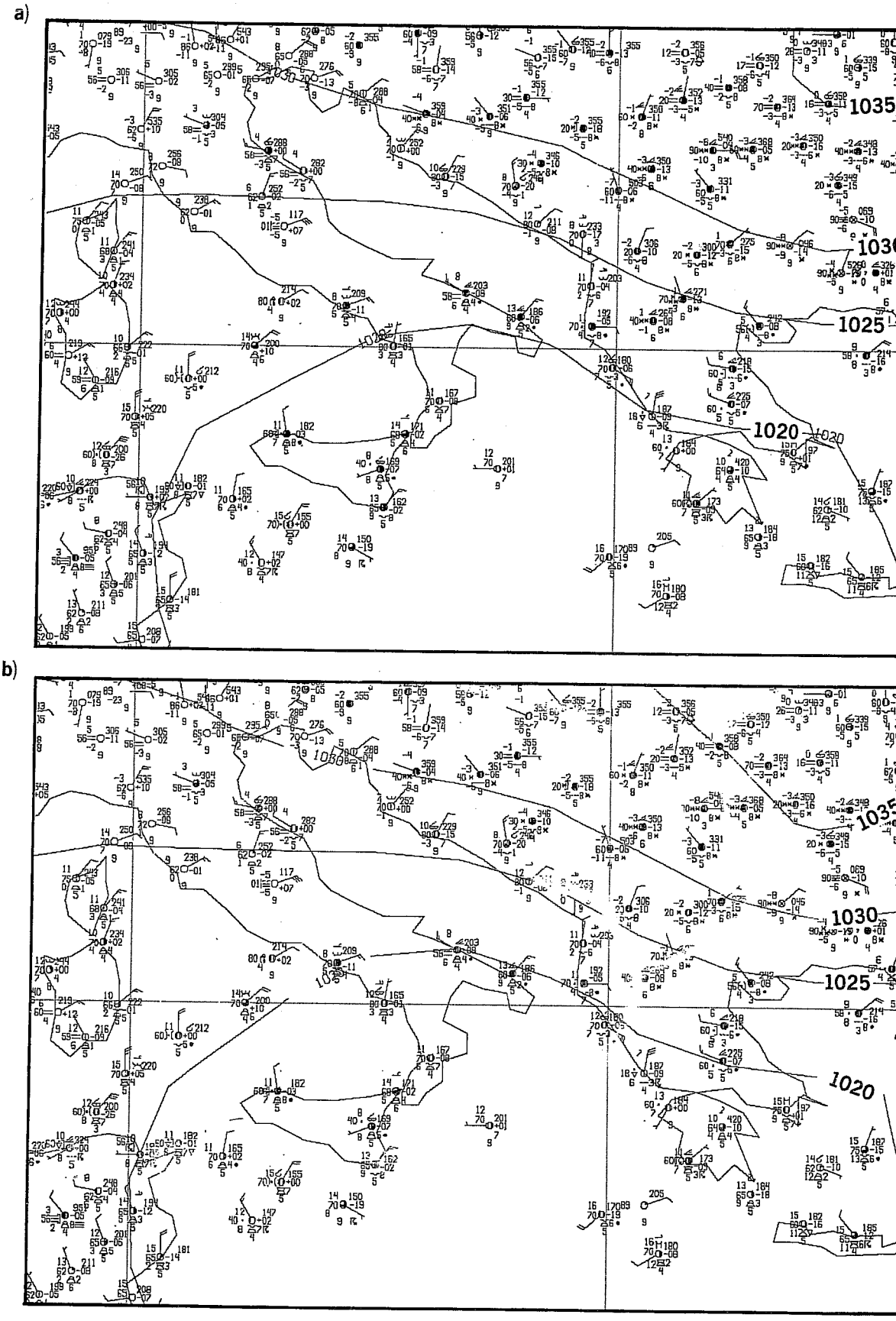

Fig. 5 PMSL field (initialised) 12 GMT, 4.12.83.
(a) including land SYNOP winds in the analysis
(b) excluding land SYNOP winds in the analysis

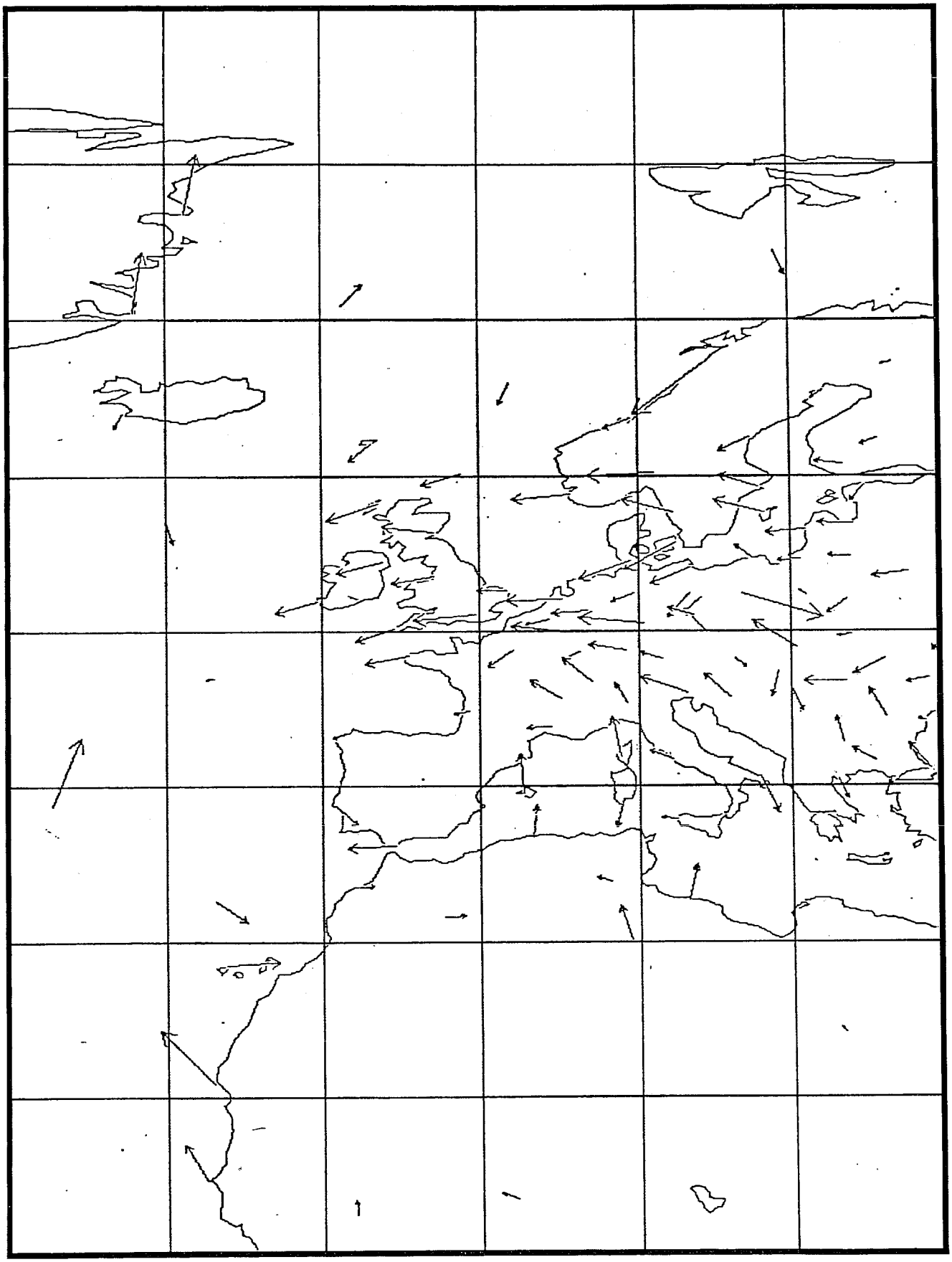

Fig. 6 Biases in (observed-first guess) 1000 mb winds for TEMPS. Based on 12 GMT data for Jan.'83. Scale 1cm = 5msec^{-1}.

seen in the two analyses over southern Italy. Exclusion of the data has led to an analysis of lower pressure, fitting the observations more closely. In addition to the surface data shown, the usual 12 GMT network of upper air data was available to the analysis with the consequence that the impact of land SYNOP wind data on this analysis would be appreciably smaller than at 06 GMT or 18 GMT. Notwithstanding the availability of the upper air data, the impact of the change on the analysis is clear.

The second error in the use of near surface data was a consequence of the preprocessing of the observations. In practice, most analysis schemes have a substantial amount of pre-analysis manipulation of observational data- e.g. adjustments to off-level and off-time data, conversion of observed quantities to more appropriate variables, cross-validation of temperatures with geopotentials, etc. Any weakness in this pre-processing can have serious consequences, and one such weakness has been found in the analyses. Statistics have been produced of (observed-first guess) 12 GMT TEMP winds for January 1983. Fig. 6 shows the chart for 1000 mb. As with the SYNOP winds of Fig. 4, large systematic errors are evident, but the cause is quite different. If a TEMP report lacks wind data at 1000 mb the pre-processing will create a value by taking the TEMP's lowest wind (provided that wind is below 850 mb) and shifting it to 1000 mbs using the first guess vertical wind gradient. Unfortunately the lowest level wind in a TEMP report is frequently its station level 10 m wind. The effect of taking this typically light wind and further modifying it by the first guess gradient is to produce a badly incorrect wind which may even suggest anticyclonic circulation around a northern hemisphere depression. This feature is severely detrimental to the analysis in (TEMP) data rich regions. It typically reduces cyclonic flow around a depression by 3-4 m/s, and has contributed to the under-analysis of surface lows in the operational analyses. Such extrapolations of multi-level data have been excluded in the revised analysis scheme, not only for these near surface levels, but elsewhere, since it was found that such extrapolation created values which had errors which were undesirable.

3. THE OI STATISTICS

The spatial interpolation from observation to grid point is done by OI (Lorenc, 1981). This technique depends heavily on the ascribed statistical properties of the various components of the system - the observation errors, normally specified according to observation type; the rms first guess errors, normally defined at all grid boxes and levels and varying in space and time; and the spatial correlations of the first guess errors and the observations. The basic quality of the analysis depends on these OI statistics - not only do they determine the extent to which the analysis fits the observations, they also play a central role in the quality control judgments (deciding whether a datum is acceptable or not is done by reference to its expected accuracy, and to its compatibilty with other observations and with the first guess). All of these statistical properties have been reviewed and revised using the assimilation statistics data base; in particular the (observed-first guess) quantities. A full account of the methods of re-evaluation are contained in Hollingsworth and Lönnberg (1984). Here some examples of their results are presented, together with a description of their effect on the analyses.

3.1 Horizontal correlations

Statistical field properties on a sphere should ideally be represented by Legendre functions. In optimum interpolation it is customary to make the usual tangent plant approximation, as the size of the individual analysis areas is usually less than 2000 km x 2000 km. The forecast error structures may then be expanded in a Fourier-Bessel series, rather than spherical harmonics. A general specification of the statistical structure of the first-guess errors requires six three-dimensional covariance functions for $\langle\phi\phi\rangle$, $\langle\psi\psi\rangle$, $\langle\chi\chi\rangle$, $\langle\phi\psi\rangle$, $\langle\phi\chi\rangle$, and $\langle\psi\chi\rangle$. Here ϕ, ψ and χ are the geopotential, streamfunction and velocity potential respectively. Assuming homogeneity of the variances, these covariance quantities can be expanded as Fourier-Bessel series,

$$\sum_{m=o}^{M} \begin{matrix}\sin\theta \\ \cos\theta\end{matrix} \sum_{n=o}^{N} f_n^m (p_1, p_2)\, J_m (k_n^m\, r/D)$$

where r is radial distance and θ azimuth. J_m is the Bessel function of first kind and order m; f_n^m is the vertical covariance function for radial mode n and azimuthal wavenumber m. k_n^m is the n'th zero of J_m'. Wavenumber m=o represents

the isotropic part of the error structures, wavenumber 1 can describe the vertical tilt of the forecast errors, and m=2 gives the ellipticity of the structure functions.

The amplitudes f_n^m of every mode for all combinations of analysis levels are determined by least squares fit to spatial correlations of observation departures from the first guess. The boundary condition for the above Fourier-Bessel expansion is that the radial derivative of the autocorrelations for ϕ, ψ and χ vanishes at a distance D. In most cases D=3000 km is sufficient to satisfy the boundary condition. For the least squares fit, the correlations between all station pairs within a distance D are required. The circular area of radius D defines the set of modes onto which the error structures of the correlation data are projected.

Efforts have been concentrated on determining the isotropic part of the six hour forecast errors. We have neglected the anisotropic modes of the Fourier-Bessel covariance model in the implementation of the revised analysis system. Preliminary results on the anisotropic components indicate that these may locally have a significant contribution to the total forecast error. The anisotropic wavenumbers will be investigated further.

Although some of the results shown in this document are based on FGGE data, the revised structure functions have been estimated from assimilation statistics from January-March 1983 over North America (60°N-30°N) and the tropics (20°N-20°S). In most of our calculation we truncated the Fourier-Bessel series expansion at radial mode N=10. The equivalent spherical wavenumber is T68. Frequently, the calculations were stable up to N=14, i.e. T96. However, in the operational implementation the correlation model is truncated at N=5 (T35) in order to gain experience with this formulation and to control noise in data sparse regions.

The radial mode n=0 is constant within the domain [0,D] and consequently describes error structures of large horizontal extent. The amplitude of the constant mode, also called the barotropic mode because of its vertical structure, was found to be larger than the total amplitude of the horizontally varying ("baroclinic") modes in the stratosphere. In the troposphere its amplitude was smaller, but still significant. As expected the length scale of the geopotential error increased with height and only the gravest modes could be determined in the stratosphere.

Fig. 7 shows the spatial correlations of (observed-first guess) between pairs of station locations, plotted at differing spatial separations. The particular variables shown is 500 mb geopotential, for a two week period in February 1979, for North American data. The computed correlations are marked by dots, with the numbers in the samples alongside. The crosses mark a truncated series of Bessel functions, fitted to the data by the method of least squares. Such a curve intersects the ordinate (i.e. at zero separation of station locations) below the 1.0 correlation point - the correlation of first guess errors is 1.0 for zero separation, but the presence of random observation errors degrades this. The variance of (observed-first guess) for the complete sample can be calculated, and using the difference from 1.0 to the zero separation correlation this complete variance can be partitioned between observation error and first guess error. In such a way revised estimates can be made of the observation errors, and of the first guess errors of the prediction model.

The Bessel function series gives a good fit to the computed correlations, and this functional representation has been used in preference to the originally specified exponential form (see Lorenc, 1981). The inability of an exponential to fit the data is shown in Fig. 8, for the same data sample as used in Fig. 7. In particular the exponential is seen to be too flat at small separation distances; a practical consequence of using such a function is that smaller scale features missing from the first guess field would not be resolved even in the presence of good and plentiful data.

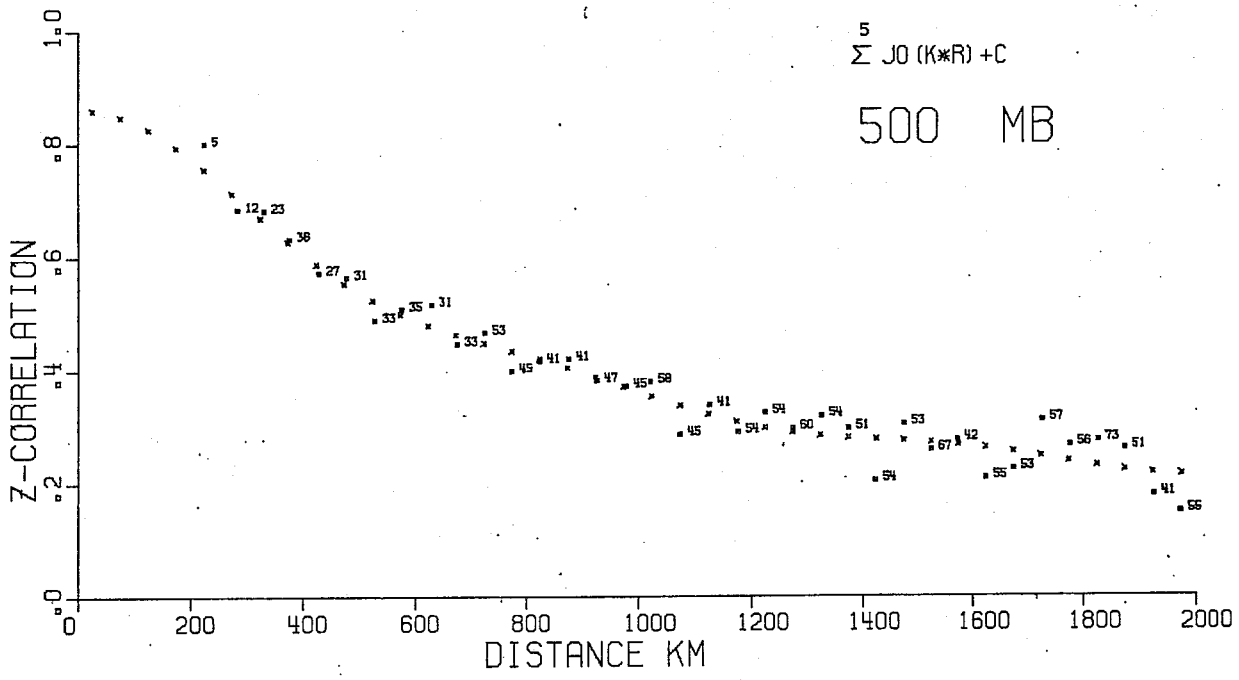

Fig. 7 Correlations of (observed-first guess) values for pairs of stations with known separation distances. The variable chosen is geopotential height at 500 mbs, for N. American data for a period in Feb. 79. Values are marked by dots, with the number in the sample plotted alongside. The crosses mark a truncated series of Bessel functions fitted to the data by the method of least squares.

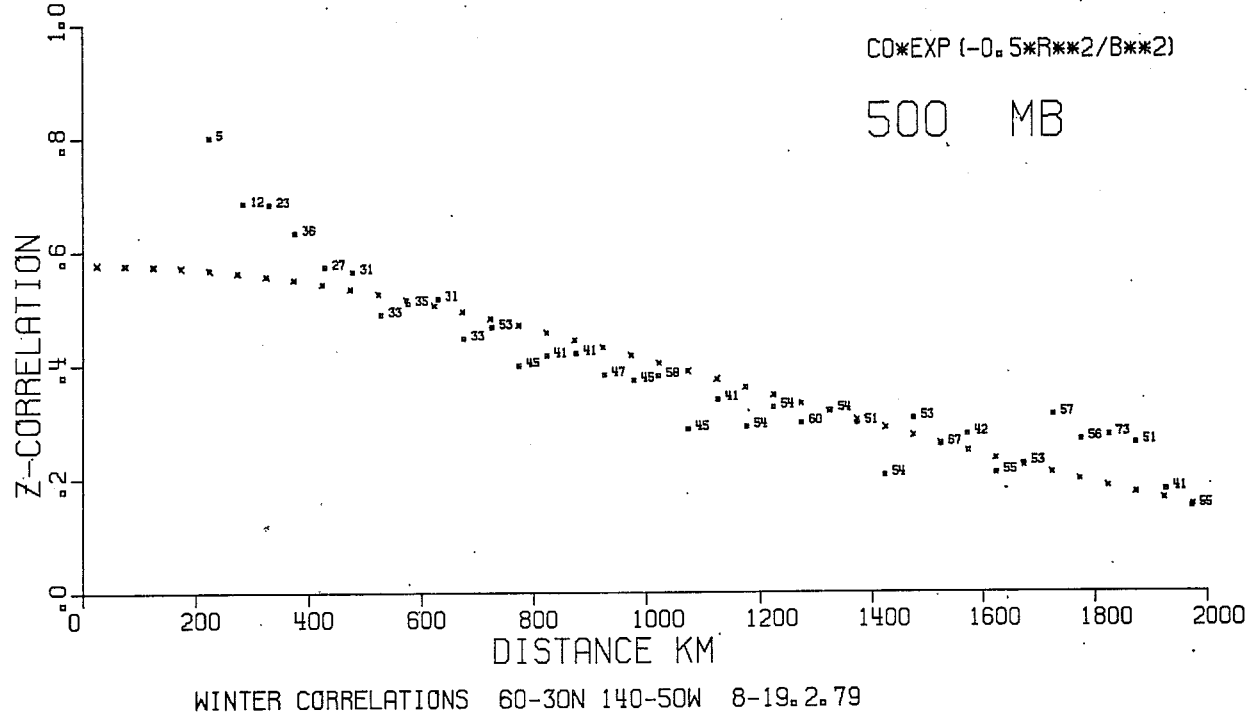

Fig. 8 As Fig. 7, but using an exponential function, rather than Bessel functions, to fit the data.

The total prediction error for the wind consists mainly of the non-divergent part. The Rossby number of the forecast erorrs, defined as the ratio of the divergent to the rotational wind components, has a minimum of 0.25 at 500 mb. In the lower and upper troposphere it reaches a magnitude of 0.4 (at 850 and 250 mb) and above 200 mb it has a value between 0.55 and 0.6. A plausible explanation of these high values in the stratosphere is the lack of proper representation of the atmospheric tides, as there was no diurnal cycle in the model at the time. The introduction of the diurnal cycle may have reduced the amplitude of the divergent wind error.

The correlation between streamfunction and velocity potential was found to be small, but there was a clear distinction between upper and lower troposphere in the sign of the correlation. However, as pointed out by Daley (1983), only correlations between ψ and χ close to unity would have an impact on the analysis.

The geostrophic coupling parameter, i.e. the height/streamfunction correlation, is an important parameter in the ECMWF statistical interpolation scheme. We have studied two aspects of geostrophy of the first guess errors:

- the correlation between the streamfunction and height fields.

- the ratio of the geostrophic winds to the streamfunction winds.

The ϕ-ψ correlation, i.e. the directional consistency between the geostrophic wind and the rotational wind, reaches a maximum of 0.92 at 400 mb. At 850 mb it has a value of 0.68 and between 700 mb and 150 mb it lies between 0.8 and 0.92. In the stratosphere it decreases to 0.7.

A significant imbalance is found between the amplitudes of the geostrophic wind and the rotational wind. This is probably a real signal as it exists at all resolved wavelengths; however it could have a contribution from errors on scales which cannot be resolved by the observation network. The analysis system underdraws the thermal winds across thin layers, while the thickness data is well drawn too. This imbalance may lead to large changes in the six hour forecast and may be related to the spin-up problem of the forecast. Further investigations into the causes of this imbalance are necessary.

The ϕ-χ correlation is weak and negative below 250 mb, while above 150 mb it is positive. Negative correlation implies convergence in lows. The positive correlation in the stratosphere may again be an indication of the missing tides.

3.2 Vertical correlations

The Fourier-Bessel expansion describes the vertical structure of each horizontal mode. For geopotential it was found that the vertical scale length decreased with decreasing horizontal wavelength. Separability is therefore not a good assumption for the height field errors. The vertical correlation of the barotropic mode is very wide and the associated temperature error is small.

In contrast to the vertical correlations of height, the variation in sharpness of the different modes of the vertical wind correlations is much smaller. Separability is therefore a much better assumption for the wind errors. The vertical structure of the divergent wind is consistently sharper than that of the rotational wind.

For the operational implementation some simplifying assumptions were made. The vertical structure of the geopotential error is described by two components; a barotropic vertical correlation for the horizontally constant mode and a mean baroclinic correlation for the horizontally varying modes. The vertical structure of the geostrophically coupled wind correlations is then described by the baroclinic correlation, as the horizontally constant geopotential component has no wind associated with it.

Apart from separating the vertical correlations into 'barotropic' and 'baroclinic contributions, the character of the new correlations is fairly similar to the old correlations in the extratropical areas. For the tropics, however, the observation studies produced a completely different picture of the forecast error structures from that assumed in the old system. The impact of the changes in the vertical height correlations are illustrated in Fig. 9, which shows the profile of the temperture change resulting from the use of a single surface pressure report, which is 5 mb deeper than the first-guess. The old system produced a very rough profile of the temperature increments with considerable changes to the stability. The rederived covariances give only modest temperature changes with a maximum at 500 mb, at which level the error of the first-guess temperature field has a maximum.

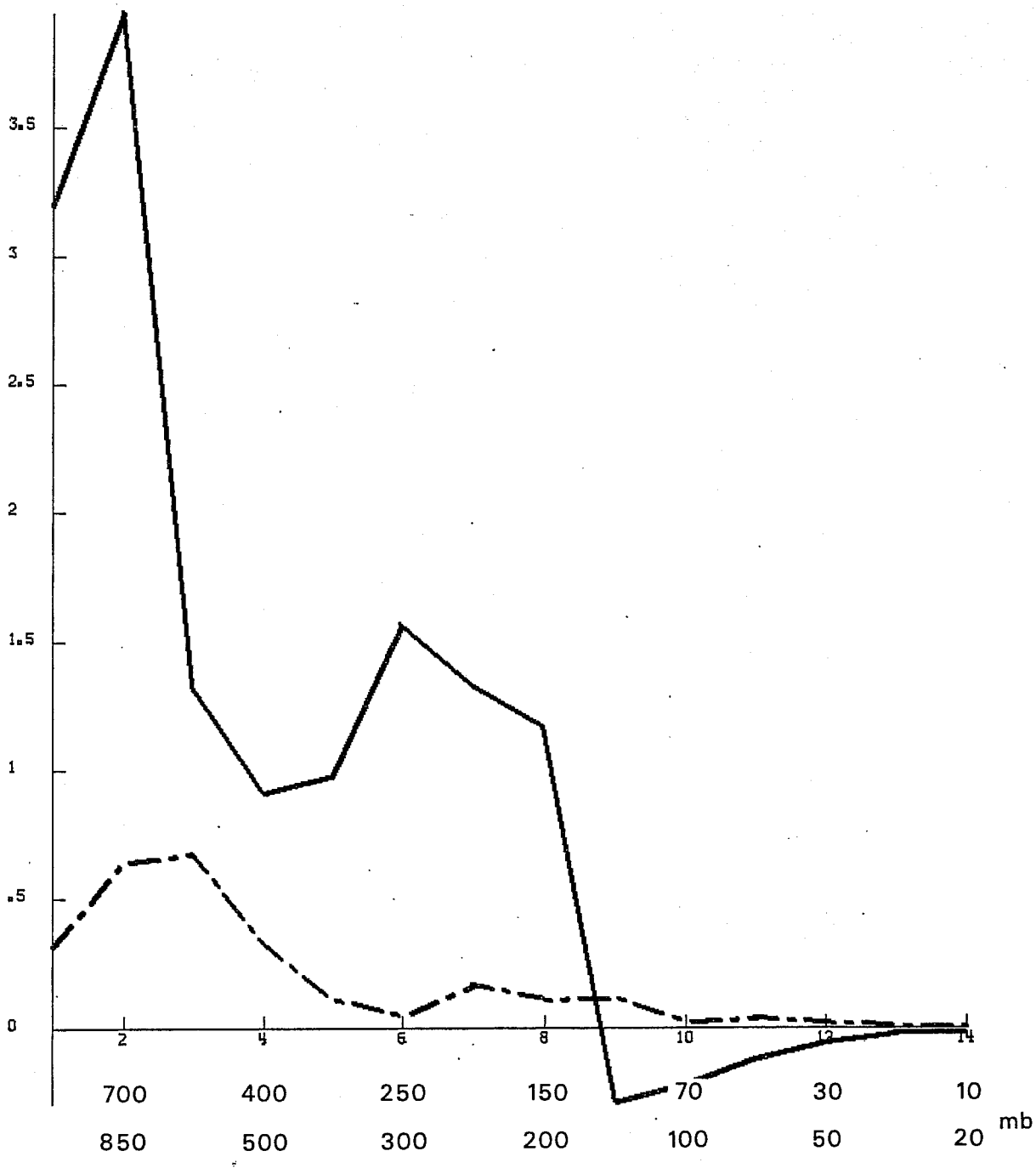

Fig. 9 The temperature increments for different analysis layers (abscissa) from one height observation at 1000 mb which is 40m lower than the first guess. The solid line is the old temperature analysis and the dashed-dotted line is for the new system.

The structure of the tropical wind errors were found to be much sharper than assumed earlier (Tables 1a and b). This decouples the upper and lower tropospheric wind analyses and the vertical smoothing which was seen in the old system has disappeared.

3.3 Accuracy of the first guess field

Returning to the estimated accuracy of the first guess field, the error partitioning technique described earlier gives a reliable measure of the mean rms error of the 6 hour forecast for a particular region (e.g. N. America). This is not sufficient for the practical application of the OI, where we need an rms error to be specified at all grid points and levels; and where we expect some temporal variability in the ascribed value - reflecting the temporal variability in observing networks which influences firstly the quality of the analysis and then, through the analysis, the quality of the subsequent 6 hour forecast. The OI technique yields as a by-product an estimate of the analysis error. The procedure in the past for generating geographically and temporally varying first guess error estimates has been to take this analysis error from the previous cycle and allow it to grow at a rate appropriate to the error growth rate of the prediction model (see Lönnberg and Shaw, 1983). The first guess error estimates derived from the assimilation statistics and described above provide a good standard against which the (analysis error+forecast error growth) algorithm can be reviewed. Two general weaknesses were found in the existing formulation. Firstly the estimated analysis error was unrealistically low in data rich regions, where an abundance of data is no guarantee of an error free analysis, particularly because of the resolution limitations of the OI statistics. (The estimated analysis error is also used in the data checking quality control check, where an OI estimate of the truth is calculated independently of the datum being checked; an unrealistic estimate of the analysis error can lead to bad judgements of the data). Secondly the assumed rate of growth of the forecast error was found to be pessimistically high for most regions, leading to an estimate of 6 hour forecast error which was generally too high. Revisions have been made as follows. The OI estimate of the analysis error now has imposed upon it a lower bound:

$$E_{a,\text{revised}} = \sqrt{E^2_{a,OI} + E^2_c}$$

where E_c is a globally specified value depending upon pressure and variable.

For the geopotential, E_c=6 m at the lowest 8 analysis levels, then increases linearly in pressure to 20 m at 10 mb. The vertical distribution of E_c for wind is similar with E_c=1 m/s in the lowest levels, becoming 4 m/s at 10 mb.

The forecast error growth rate is assumed to be linear in time, growing to a random error state ($\sqrt{2}$ of the climatological variance) in 6 days in the extra-tropics and in 2 days in the tropics, with a transition zone between the regions. This formulation provides a coherent picture of how the system performs - the error growth rates match reasonably well the generally accepted limitations of predictive skill of the Centre's current model. Starting from the revised estimate of analysis error we arrive at a 6 hour forecast error which is in good agreement with the statistical estimates in those regions where evaluations of the latter have been made. The magnitude of the change to the first guess error estimates can be seen in the examples shown in Fig. 10(a) and (b). These show the old and new error estimates for 500 mb geopotential height for the same occasion (a 12 GMT cycle), chosen at random. The new estimates are approximately half as big as the old values in middle and high latitudes; in the tropics the reduction is more modest. The new values are similar in magnitude to the generally quoted rms error estimates of TEMP geopotentials - the 6 hour forecast of the Centre's assimilation system is quite accurate, emphasising that current assimilation techniques merit the need for observing networks that are both accurate and well distributed. Another point of note in the revised estimates is that there is generally little geographical variation in the first guess errors; the modest maximum over Northern Africa is a reflection of the absence of data in that particular region in the preceding assimilation cycle.

3.4 Observation error statistics

The ascribed observation error statistics have also been revised, see Tables 2(a) and (b). These revisions are based on the partitioning of the error as described earlier for the TEMP data; the PILOT revisions are made to follow these; the changes to the SATOBS and AIREP data are not based on such a detailed investigation, but are made on the evidence of day to day measures of the fit of the data to the first guess and analysed states; and the PAOB revision has been considered separately, as discussed below.

The component wind errors of TEMP(and PILOT) have been substantially reduced in the middle and upper troposphere and stratosphere. The need for this was

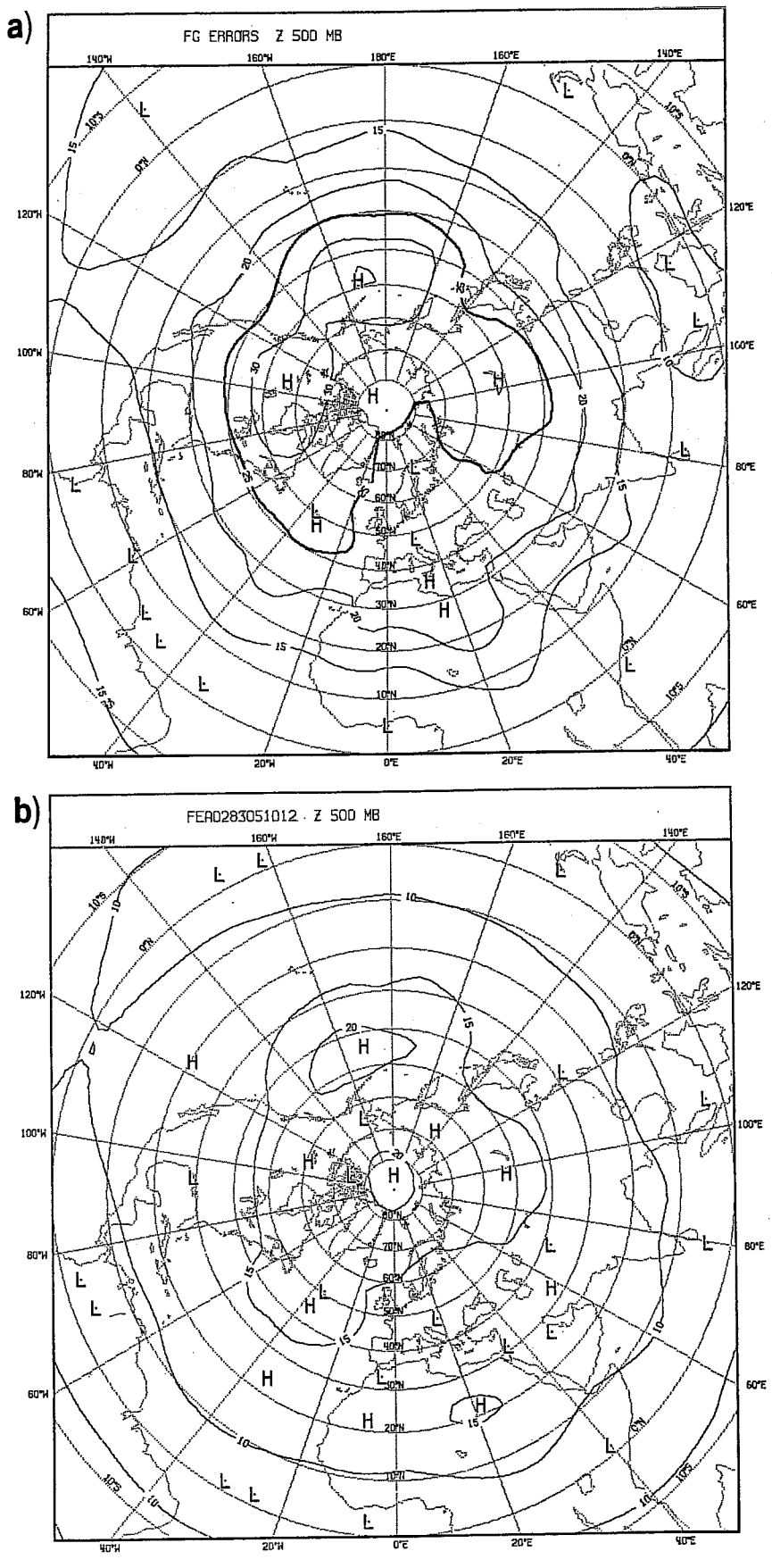

Fig. 10 Ascribed first guess RMS error estimate for 500 mb geopotential height (m), for 12GMT 31.8.83 (a) old system (b) new system.

evident from the realisation that the original value of approximately 6 m/s exceeded even the rms of the departure of observed value from first guess estimate - a measure which includes both observation and model error. The revised estimate of 3-4 m/s for the upper tropospheric region is reasonably consistent with independent estimates of TEMP wind errors. In the lower troposphere the TEMP/PILOT wind errors have been modestly increased; this is reassuring in the sense that the old assimilation system had an undesirably high rejection rate of near surface winds from TEMPS and PILOTS - so much so that approximately half of the ascents which were flagged as containing rejected data were ascents where either the 850 mb or the 700 mb wind had been rejected. This is not in accord with normal subjective experience - the majority of TEMP errors are not in their low level winds. The increase in ascribed error will increase the tolerances of the quality control checks, and should therefore yield a more acceptable flagging rate of such data. For TEMP geopotential errors, the revised values are modest reductions of the earlier values in the troposphere, with quite substantial reductions in the stratosphere. The errors for SATEMS remain unchanged; these were revised fairly recently in the operational system and they are considered to be quite appropriate; the values correspond to those proposed by Phillips(pers.comm). The SATOBS errors have been merged so that a distinction between the three available systems is no longer made; a general reduction has been made which will cause these data to have a greater impact in the analyses. In the old system such data had only a very modest impact, and frequent examples had been noted where such data were clearly wrong but, because of the high ascribed errors,remained undetected by the analysis. Similarly no distinction is made in the new system between AIREP and ASDAR aircraft wind reports, primarily because the assimilation statistics have not been evaluated for such mobile platforms; however there was a clear need, from the evidence of day to day measures of fit that the conventional AIREP data was more accurate than had previously been thought, and in reducing these values to more appropriate levels we have taken the same error levels for the ASDARS, for which the changes are seen to be generally small.

Perhaps the most dramatic change in ascribed error levels is that of the PAOBS (the subjectively derived estimates of surface pressure produced by

WMC, Melbourne for the southern hemisphere and disseminated twice daily on the GTS). The ascribed rms error has been increased from 14 to 32 m. This has a very substantial impact on the southern hemisphere analyses, as will be shown later. That there is a need for such a high error level is suggested in Figs. 11 and 12. These show histograms of the (observed- first guess) values for SYNOPS and for PAOBS respectively for a one month sample of 12 GMT analyses. Only data considered for use in the analysis have been included; thus PAOBS north of 19°S or over land regions are excluded. The striking difference in the two histograms is the spread of the departures as evidenced in their standard deviations (19.6 and 40.7 m, respectively). The geographical distribution of the two observing networks are not the same - the PAOBS are spread more uniformly over the extra-tropical southern hemisphere than are the SYNOPS, which are concentrated in the land regions, and so it is not valid to ascribe the difference in distributions entirely to the difference in accuracy of the two observation types. Nonetheless there is a clear implication that the PAOBS have a substantially higher error level than the SYNOPS. The SYNOP error is known with good accuracy - it is approximately 7 m. Partitioning the standard deviation into components this suggests the first guess error, for the sampling region of the SYNOPS, is approximately 18.5 m. This is probably inappropriately low for the region covered by the PAOBS. However even if the estimated first guess error is increased to 30 m (a value which is consistent with that derived by the analysis error plus forecast error growth algorithm), it still yields an estimated error for the PAOBS of approximately 32 m. The consequences of such a revision of the PAOB error estimate is two-fold. Firstly the data has much less impact on the analysis (e.g. a coincident SYNOP and PAOB would now have relative weights in the analysis of 20:1). Secondly the rejection rate for PAOB data should drop; this is desirable in the sense that the old system rejects PAOB data more frequently than any other source of single level data, a further suggestion that the old ascribed error level is inappropriate.

4. QUALITY CONTROL CHECKS

The importance of good quality control procedures within an analysis is well known. In the ECMWF analysis there are currently two main means of identifying an incorrect datum. The first is a check against a first guess

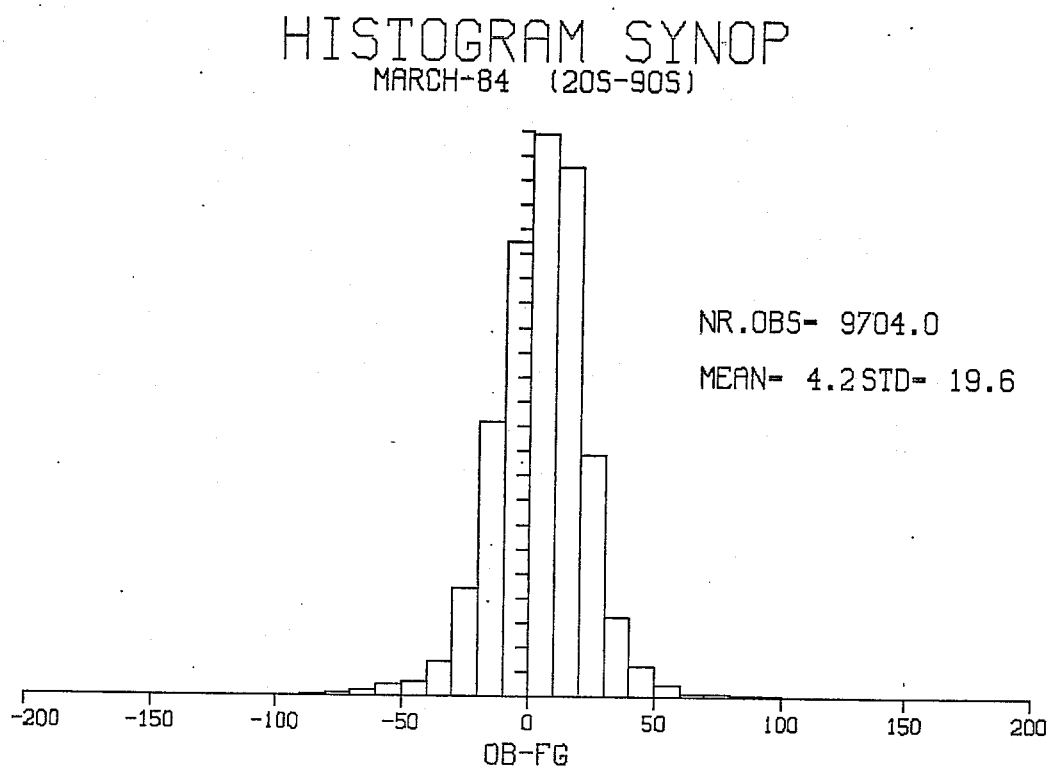

Fig. 11 Histogram of (observed-first guess) surface pressure values (converted to geopotentials) for SYNOP reports south of 20° S for March 1984 (12GMT datum time). Units : metres. The markings on the vertical scale are in units of 100 reports.

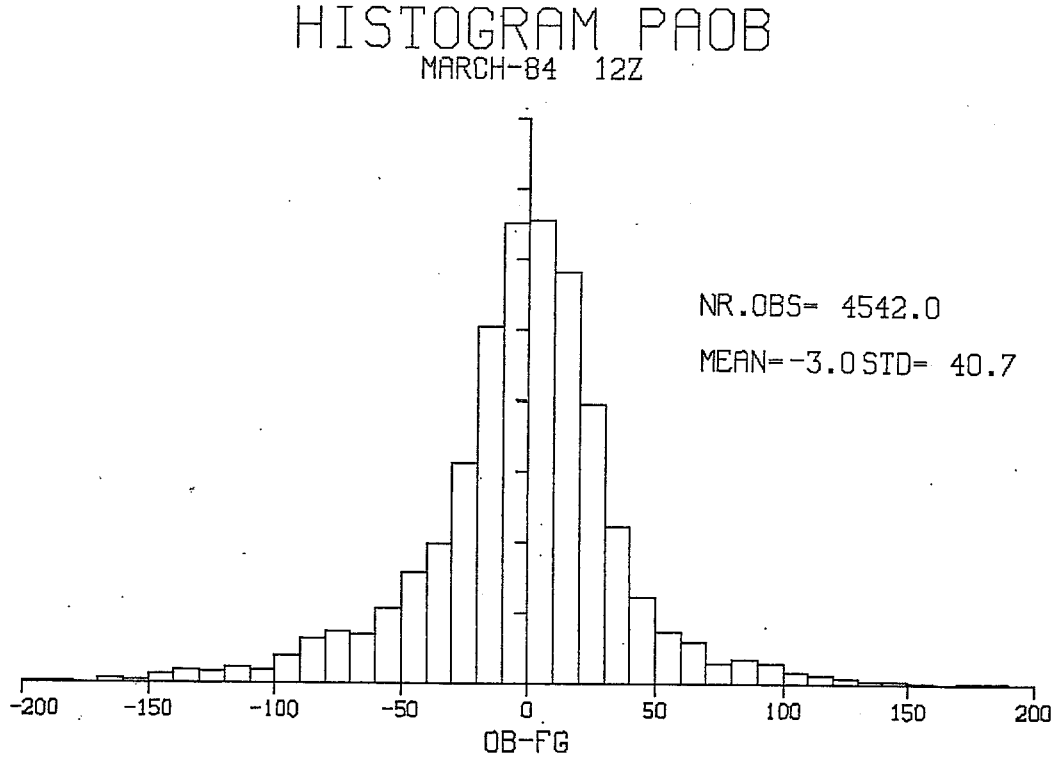

Fig. 12 As Fig. 11, for PAOB reports.

value; the second is a preliminary OI analysis which uses surrounding data, and the first guess value, to produce an independent estimate of the datum, against which the datum is then checked. The tolerances permitted depend on the ascribed rms observation error; the estimated rms error of the field value being used; and a multiplicative, empirically determined, tolerance factor. The first guess check, for example, is

If $\delta^{o^2} > (1 + \varepsilon^{o^2})\ \text{ERRLIM}_j$ then flag = j

where ERRLIM_{1-3} are 16,36 and 64.

The quality control flag can take on values of 0(correct); 1(probably correct); 2(probably wrong); and 3(wrong). Ultimately data flagged 2 or 3 are rejected. These checks are known from operational experience to be unsatisfactory. Two striking weaknesses are that of the flagged TEMP reports approximately half are flagged because lower tropospheric winds are judged to be wrong by the data checking step (as already mentioned); and in the upper troposphere individual reports of geopotential or wind are capable of producing analysis increments which are impractically large. These two weaknesses indicate the need for a relaxation of the quality control checks in some respects, but a tightening in other respects.

The assimilation statistics package provides some objective guidance. An example is shown in Fig. 13. It shows the histogram of (observed - first guess) differences for USA TEMPS at 500 mb for the 12 GMT analyses for May 1983. The distribution is sharply peaked, with very little bias, suggesting that both observations and first guess are highly reliable. As regards the quality control checking, given that the estimate of first guess rms error varies little from one day to the next (for a given time of day, and with a regular receipt of data), the original quality control bounds beyond which data would be flagged 1,2,3 by the first guess check can be represented by the vertical lines drawn above the abscissa in Fig. 13. It is seen that for all ascents making up the sample (approximately 3000) the first guess check

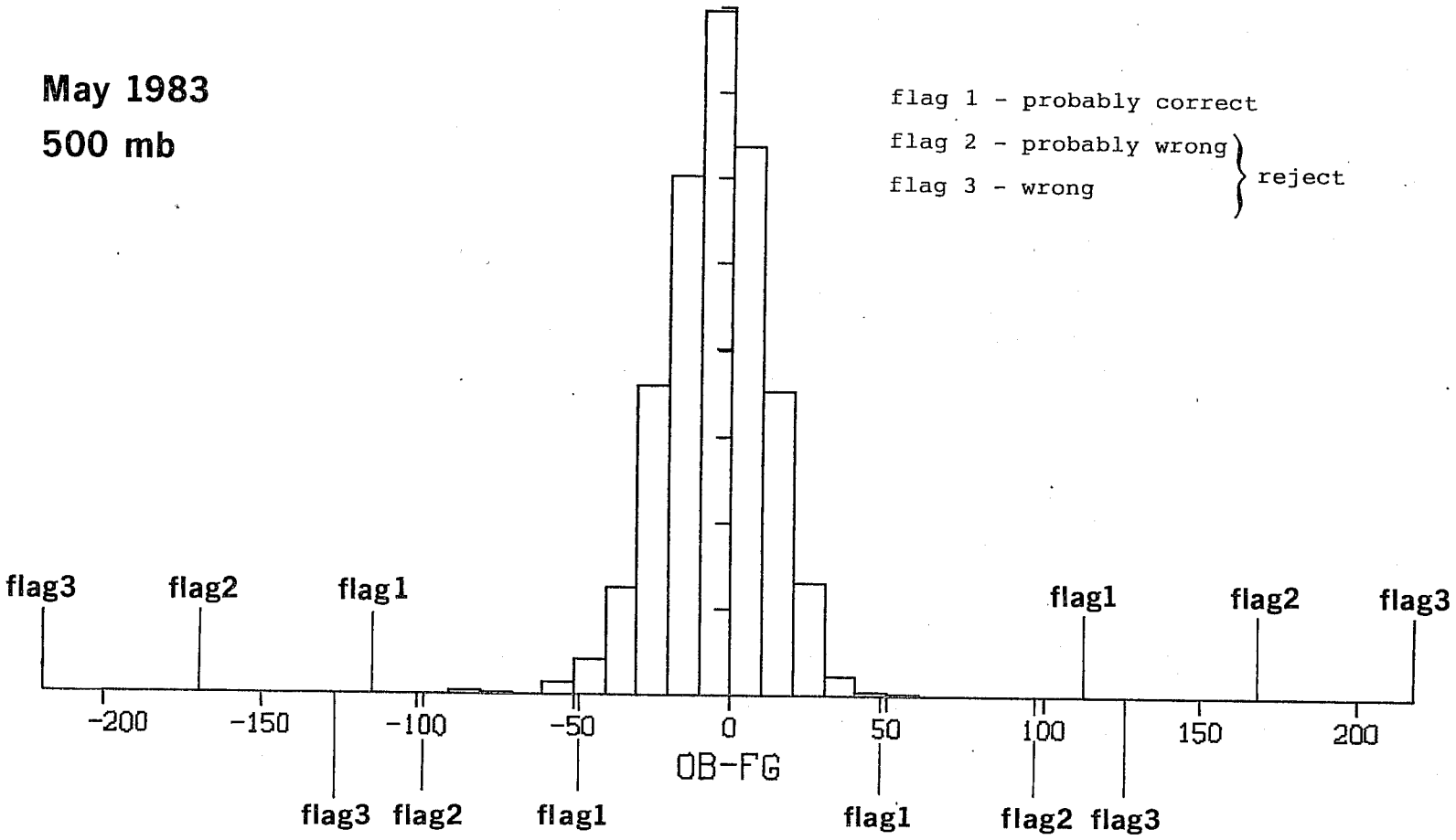

Fig. 13 Histogram of (observed - first guess) 500 mb height values for N. American TEMP reports for May 1983 (12 GMT datum time). Units : metres. The markings on the vertical scale are in units of 100 reports.
The old flags are shown above the abscissa and the new ones below.

did not raise a single flag; and that the first guess check could be tightened considerably, as an aid to identifying the occurrences of incompatibility not found in this particular sample.

The changes to the tolerances which stem from the revision of the OI statistics are such that generally the tolerances are tightened, and so the need to change the values of ERRLIM, and other components of the tolerances, is reduced (the relaxation of low level TEMP/PILOT tolerances is an exception). However some changes have been judged desirable, and these are now described. The value of ERRLIM for j=1 has been changed from 16 to 9. This in itself does not lead to a change in rejections since it only increases the likelihood of a flag 1 setting on a datum. However a new quality control test has been added which exploits this flag1 setting in a particular way. It is frequently found that multi-level reports, most noticeably TEMP geopotentials, have considerable departures from the first guess at several successive levels; if such data, which is usually incorrect, is not rejected at the first guess check, there is the possibility of it surviving the subsequent data checking step, since the data at successive levels support each other. The new quality control check examines the flags raised at successive levels immediatedly after the first guess check; if four or more successive levels have a flag of 1 or more for a particular variable, then those data are rejected; in the case of geopotentials, all data at levels above these levels are also rejected, since such geopotentials will have typically undergone stringent tests confirming their hydrostatic consistency with the incorrect data below. To make this new quality control effective the stringency of the flag1 setting has been increased, reducing ERRLIM from 16 to 9 for j=1. With this revision to the tolerance algorithm, and with the OI statistics revision, new limits of the first guess check have been marked in Fig. 13, as vertical lines below the abscissa. As before,the revised first guess checks do not encroach on the actual distribution of departures - nor should they in this well behaved sample, but the tightening of the test is clear and can be expected to have an impact on other, less accurate, samples of data.

The estimated first guess error variance has a geographical dependence, reflecting the density and accuracy of the data used in the preceding analysis cycle, and the rate of forecast error growth. For a particular type of observation,variable, and level,maps of first guess error tolerances can be produced, using appropriate first guess error distributions.. This has been done for both the old and the new system, see Fig. 14(a) and (b). This shows the two estimates of the flag3 first guess check tolerances, for SYNOP pressure reports, the tolerances being quoted in geopotential metres. An observation whose departure from the first guess exceeded the tolerance shown at the location of the observation would be rejected by the analysis. In both the old and the new systems the maximum tolerance is in mid-Pacific, where confidence in the quality of the first guess pressure is a minimum. However the new system permits a maximum departure of approximately 130 m from the first guess field (compare with 225 m in the old system). The lower value is more appropriate; errors in the first guess field are rarely as large as 17 mb.

Another revision of the tolerance factor ERRLIM which was deemed necessary was in the first guess check of winds. The two components u and v are checked together:

$$\text{If} \quad \left(\frac{\delta o_u^2 + \delta o_v^2}{2}\right) > \left(1 + \frac{\varepsilon o_u^2 + \varepsilon o_v^2}{2}\right) \text{ERRLIM}_j \text{ then flag} = j$$

If an error is concentrated entirely in one component of wind that error has to be twice as large, in terms of standard deviations,as a geopotential error before a quality control flag is raised. To correct this anomaly the revised ERRLIM for winds are half those for geopotential, i.e. 4.5, 18 and 32.

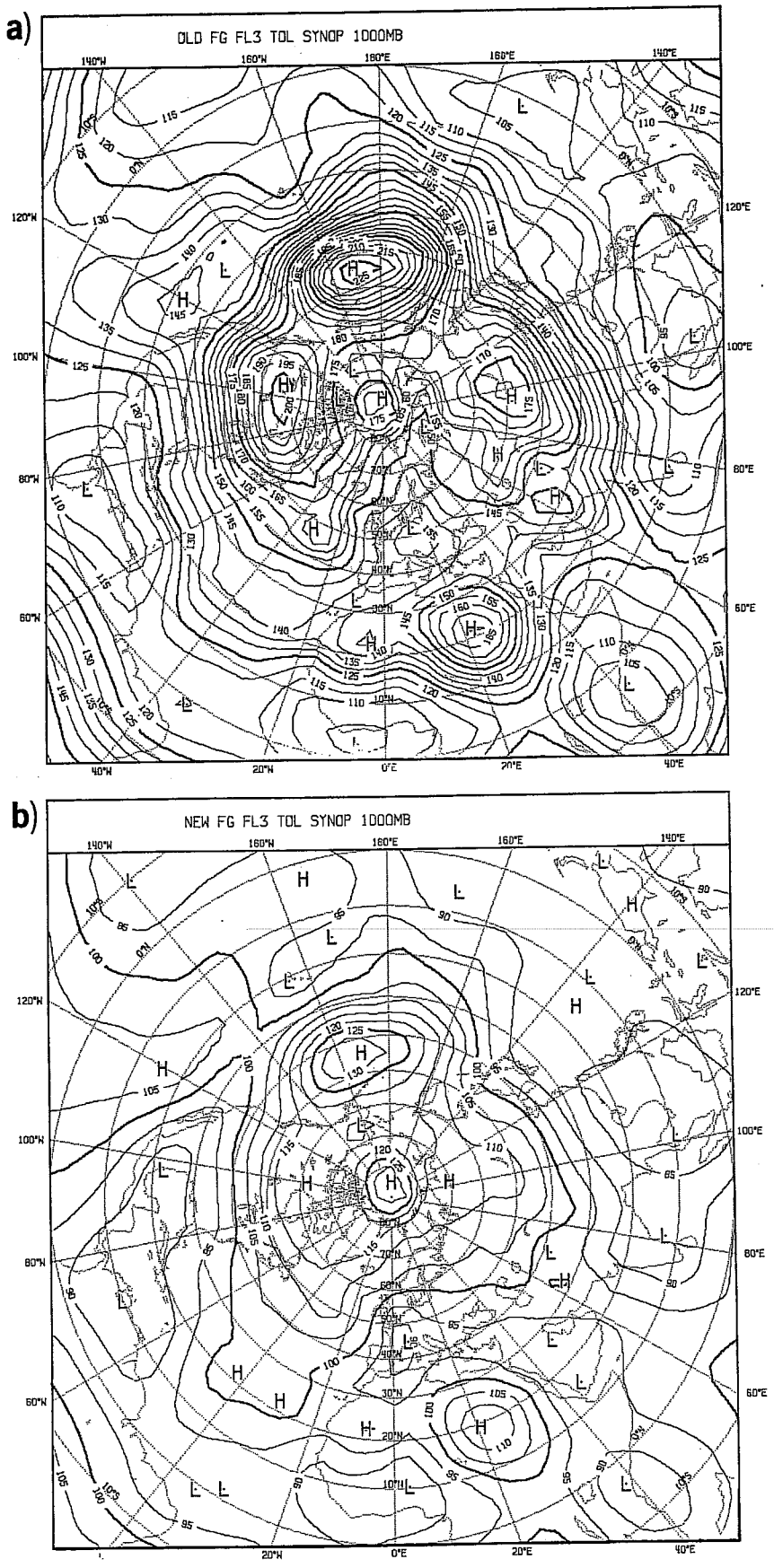

Fig. 14 Tolerance limits of the 'flag 3' first guess check for SYNOP pressure observations. (Limits expressed in geopotential metres, and applied in the context of a 1000 mb geopotential height analysis). (a) old system (b) new system.

5. THE ANALYSIS OF UPPER LEVEL GEOPOTENTIALS

As already mentioned in Sect.2, the vertical depth of the atmosphere is split into three separate slabs where there is sufficient observational data to require separate analysis of these three layers. The data selections for the three slabs differ, but some commonality is possible in levels close to the slab boundaries. In practice this overlapping of data selections may still be insufficient to guarantee smooth transitions, in terms of analysis increments, as one proceeds from one slab to the next. The most serious consequence is found in the vertical profile of geopotential increments, where a discontinuity across a slab boundary transforms to an erratic profile of temperature increments, when the post-analysis vertical interpolation to model coordinates and variables takes place. An ultimate solution to this problem is to avoid the vertical partitioning of the atmosphere, and have a common data selection throughout the full depth of the atmosphere. This is not feasible within the framework of the current system, given the constraints on matrix size and the excessive size of the horizontal boxes in data rich regions. An alternative which mitigates the effects of the discontinuity, is to replace the analysis of geopotentials in the two upper slabs by an analysis of geopotential thickness. By using the bottom slab to provide a reference level, one is effectively permitting the plentiful near-surface data to have an impact on the geopotential structure in the upper slabs without the data being explicitly used in those upper slabs. Such an approach has been incorporated in the revised scheme. The possibility of extending the technique to include the wind analysis was investigated. Discontinuities in the wind arising from the different data selections are more modest than for geopotential, and no clear benefit was achieved in the analysis. Consequently the process is restricted to geopotential thickness. An example of the benefits is seen in Figs. 15(a) and (b) which show the 850-700 mb thickness (expressed as layer mean temperature) from analyses with and without the revision, respectively. Also plotted on the diagrams are observed layer mean temperatures, most of which are SATEM reports (as indicated by the identifiers 33,34). The area of greatest difference is at 50°N, 30°W where the new analysis is warmer by approximately 2°C, fitting the observed values better.

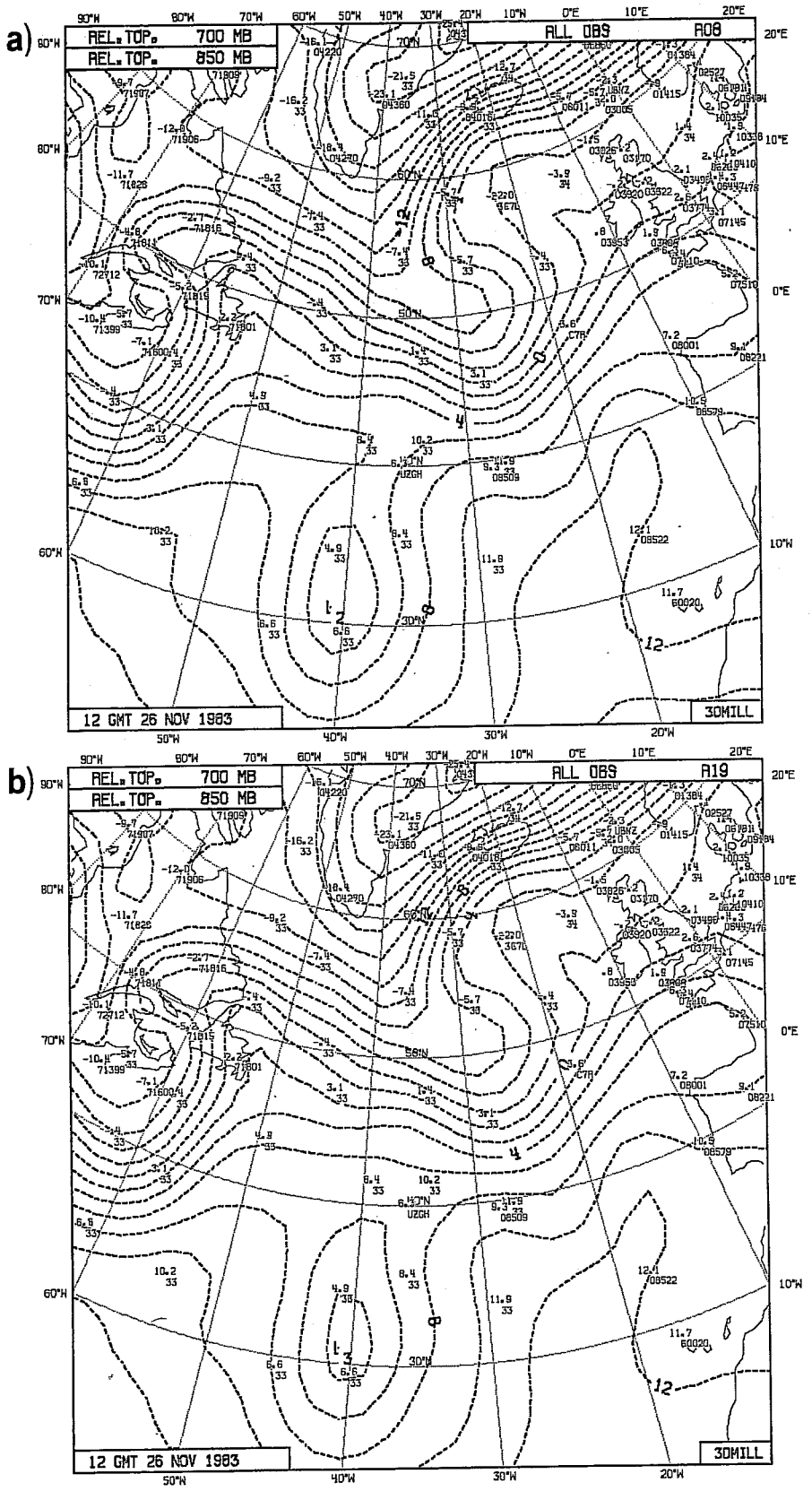

Fig. 15 Analysed layer mean temperature, 850-700 mb, for 12GMT, 26.11.83. Units ^{o} C. Analyses based on (a) geopotential height, (b) geopotential thickness.

6. THE IMPACT OF THE CHANGES ON THE ANALYSES

The effects of the various changes described in the preceding sections have been examined by the repetition of assimilation sequences for selected periods, using as a baseline the Centre's operational assimilation (these operational assimilations were in certain cases reruns of the original operational sequences from which incidental system modifications were excluded, ensuring satisfactory intercomparisons of the new analysis system with the old analysis system). Three periods have been examined: 4-10 May 1983; 24 Nov-4 Dec 1983; and, in semi-operational mode, 7-22 May 1984. In the first of these three periods, the 8 days of assimilations were successively repeated, introducing certain elements of the changes in turn - first the revision of the quality control tolerances and first guess errors; then with the addition of the revised horizontal and vertical structure functions; and finally the modified data selection and data usage algorithms. For the other two periods, the full set of modifications (including the introduction of a thickness analysis in the upper slabs) were tested together. The first two days of the first two periods can be regarded as a settling-in phase when the system was adjusting to the drastic revision of first guess errors; for the third period it was possible to avoid this phase by using appropriate first guess errors from the start. In addition to these three periods, shorter period experiments were run on specific case studies. A total of approximately 30 days of assimilations are available for study. The results presented here are drawn from different periods within the experimental sequences and are intended to be a fair documentation of the more important changes brought about by the revisions.

The quality of the assimilations can be measured in various ways. Perhaps the most important are the ability to fit the observational data with appropriate accuracy; the efficacy of the quality control judgements; the quality of ensuing forecasts; and the relative roles played in the assimilation by the prediction model, the analysis and the initialisation. Here, each of these four measures are examined; the order in which they are presented reflects not the order of importance of the evaluations but rather a logical sequence. The first aspect in particular, namely quality control, forms a foundation on which the remaining evaluations are built.

6.1 Quality control

The table below summarises the global rejection rates of the various types of observations, averaged over 7 days of 12 GMT analyses for both the old and the new analysis system (Akylidiz, pers.comm.). A rejection here is indicative of quality control rejection within the analysis of at last one datum in the observation; it does not imply complete rejection of the observation.

Comparison of average rejection rates for 7 12 GMT analyses
for 7 12 GMT analyses (7-13 May 1984)

	Old	New
SYNOP/SHIP	76.3	67.4
TEMP	41.7	65.7
PILOT*	14.3	4.4
AIREP	2.6	5.8
SATOB	0.4	1.7
DRIBU	1.6	1.4
SATEM	0.7	0.6
PAOB	5.7	1.6

*PILOT evaluations based on the preceding 06 GMT analysis; at this earlier time the increased number of PILOTS give a better sample.

Rejected data are not necessarily common to both systems, and so the above table understates the actual differences in quality control judgements of the two systems. Nevertheless, substantial changes are clear.

The total numbers of SYNOP/SHIP observations with a rejected datum are reduced in the new system, despite the fact that appreciably more SYNOPS are presented to the analysis by virtue of the data selection changes. The great majority of SYNOP rejections relate to the pressure element rather than wind; a few of the rejections in the old system would be for land SYNOP winds, now discarded in the new system. The overall reduction in rejection rate is judged to stem from the sharper OI structure functions, and from the ability to more correctly resolve strong pressure gradients by virtue of the exclusion of land SYNOP winds and TEMP wind extrapolations.

The number of TEMPS with rejected data in the new system is much higher than in the old. This is mainly caused by the new multi-level check, acting in particular on TEMP geopotentials. The difference in the two numbers would have been greater were it not for the new system rejecting fewer low level winds. This latter feature is also found in the reduced number of PILOTS now with rejected data; as discussed earlier, a weakness of the operational system was its excessively stringent limits imposed on low level wind data and it is gratifying to see this feature improved in the new system. Returning to the multi-level check, Fig.16 illustrates the type of judgement it makes. It shows a 100 mb initialised analysis of geopotential height for 12Z 10.5.84. The analysis is based on the original, operational system. The multi-level check in the new system led to the rejection of three geopotentials within the region shown; these three values are circled in the figure. (Other data on the chart may have been rejected by both systems; here we are concerned solely with the mult-level check). Although the old analysis accepted the data, it is clear that the (initialised) field cannot accommodate the values presented and used in the analysis, and rejection of such data by the new analysis is, therefore, justified.

A modest but appreciable increase in the number of rejected AIREPS and SATOBS occur with the new system; previously such data had to be grossly wrong for the analysis to recognise it as such.

The small volumes of DRIBU (drifting buoy) pressures available to the analysis are insufficient to give more than an impression of the relative performance of the two systems; rejections are typically similar (often associated with individual buoys which are repeatedly, and grossly, wrong), but judgements differ on some occasions.

SATEM data were judged to be highly reliable by both systems during the period considered.

The new system rejects a much lower proportion of PAOBs than does the old system, giving a percentage rejection rate which is more comparable to the rejection rates for other forms of single level data.

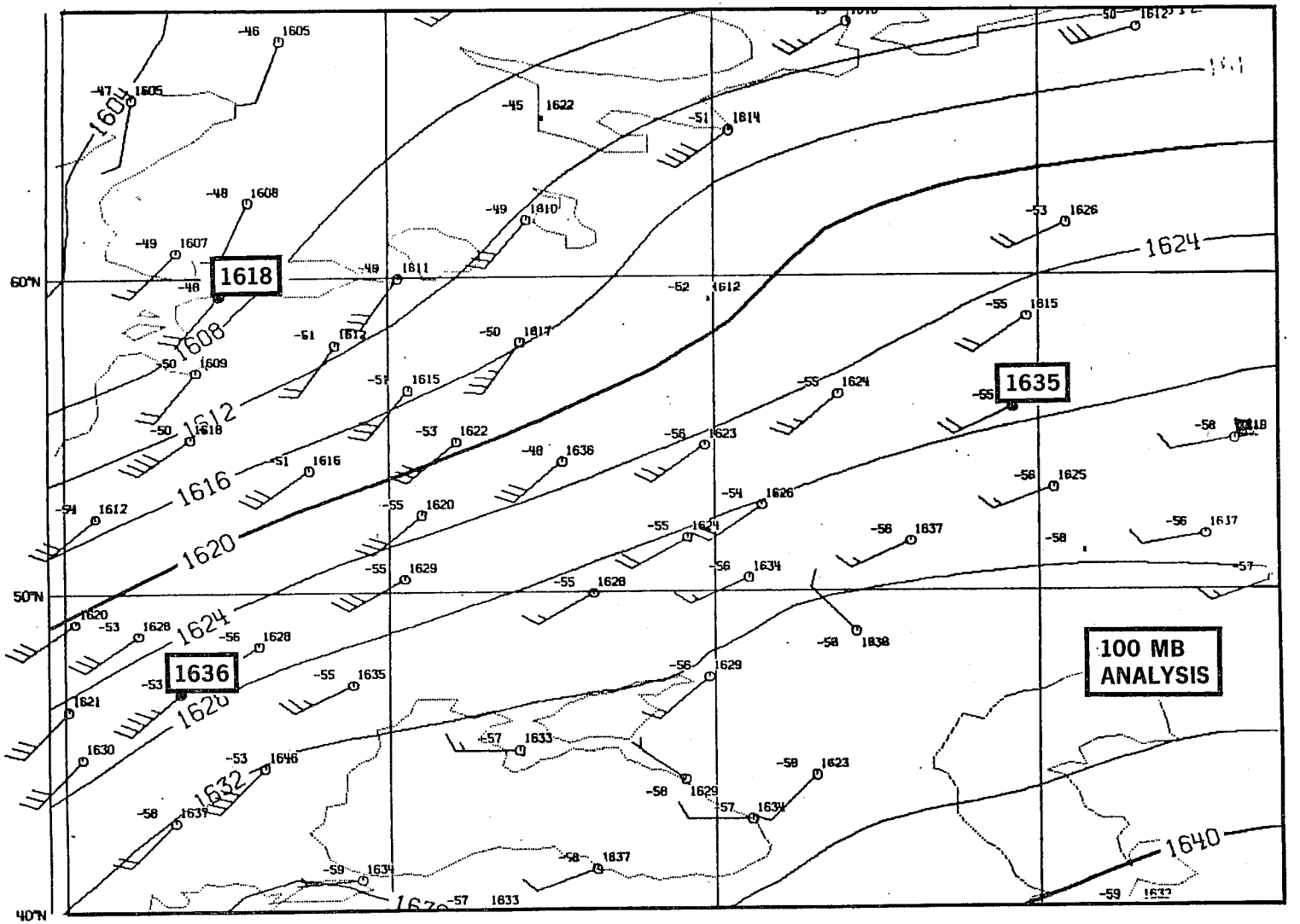

Fig. 16 100 mb geopotential height analysis (initialised) 12GMT 10.5.84. The analysis is based on the old system. The three geopotentials ringed were accepted by the old system, but rejected in the new.

In summary the new system is making a substantially different discrimination to the old system of correct and incorrect data, with both increases and decreases in rejection rates depending on data type. The question remains whether the new discrimination is better. Ultimately such a judgement is subjective. The November 1983 sequence was partly chosen for study because in the course of operational working, the Centre's analysts had documented numerous cases of bad quality control judgements. The new system was seen to correct approx. 80% of such judgements, failing to change the remaining 20%. Evaluated over the full 30 days of available assimilation, the overwhelming subjective impression is in favour of the new system - where different quality control judgements have been made, the new system almost invariably has made the better judgement. Deficiencies still exist of course, and further means of improving the quality control screening of observational data need to be pursued in future.

Finally, to help demonstrate the efficacy of the new system's quality controls, one example is included here. Fig.17 shows a plot of SYNOP data for 12 GMT, 9.5.84, together with a chart of the operational first guess mean sea level pressure field. A clear data problem exists, in that some observations (circled) have been presented to the analysis which are quite at odds with both the first guess field and with adjacent data. We can be further confident that this batch of data is incorrect in so much as they lack time continuity with preceding and subsequent reports. The origin of the incorrect data is not known and is irrelevant to our discussion. The then operational system (i.e the old system) accepted the data, producing a quite un-meteorological analysis increment field of 1000 mb geopotential height, see Fig.18(a). Changes of more than 100 m are imposed on an increment field with values of typically 10 m or so. The corresponding increment field for the new system is shown in Fig.18(b) - the revised quality control checks have succeeded in rejecting all the incorrect observations in the region in question.

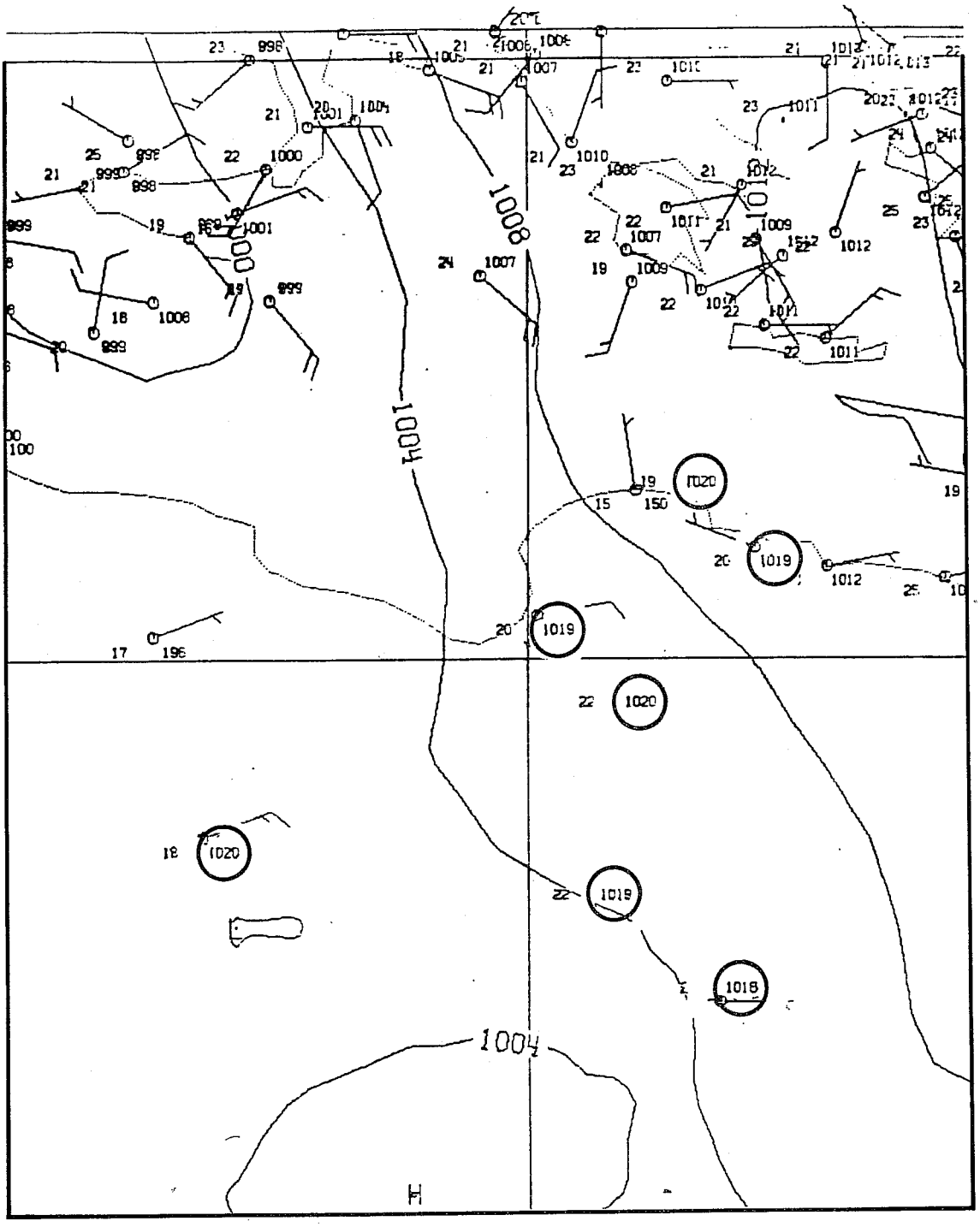

Fig. 17 First guess PMSL field, and SYNOP reports, 12GMT 9.5.84. The observations circled are incorrect.

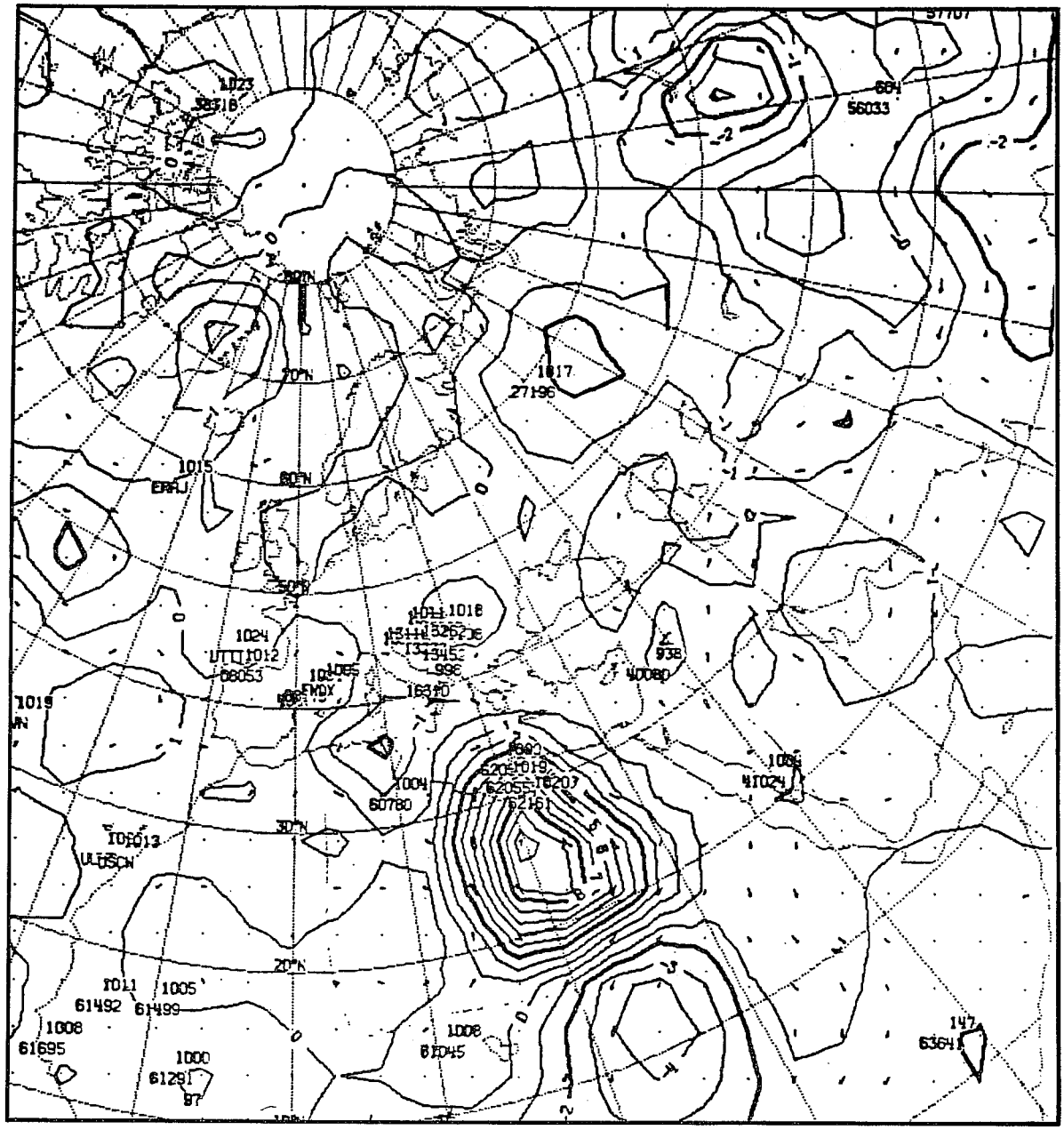

Fig. 18a 1000 mb geopotential height analysis increment, 12GMT 9.5.84. Units = m. Old system.

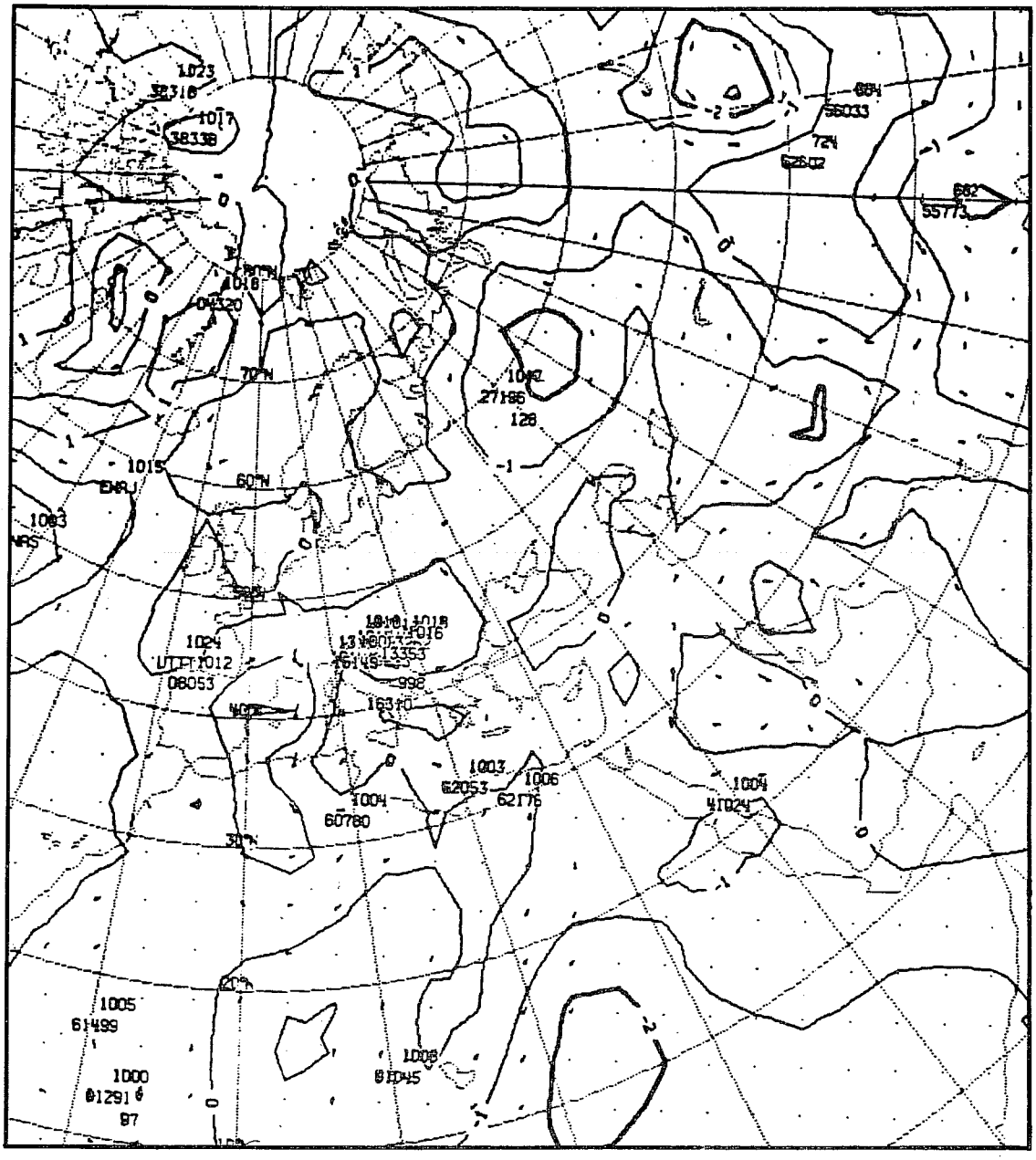

Fig. 18b 1000 mb geopotential height analysis increment, 12GMT 9.5.84. Units = m. New system.

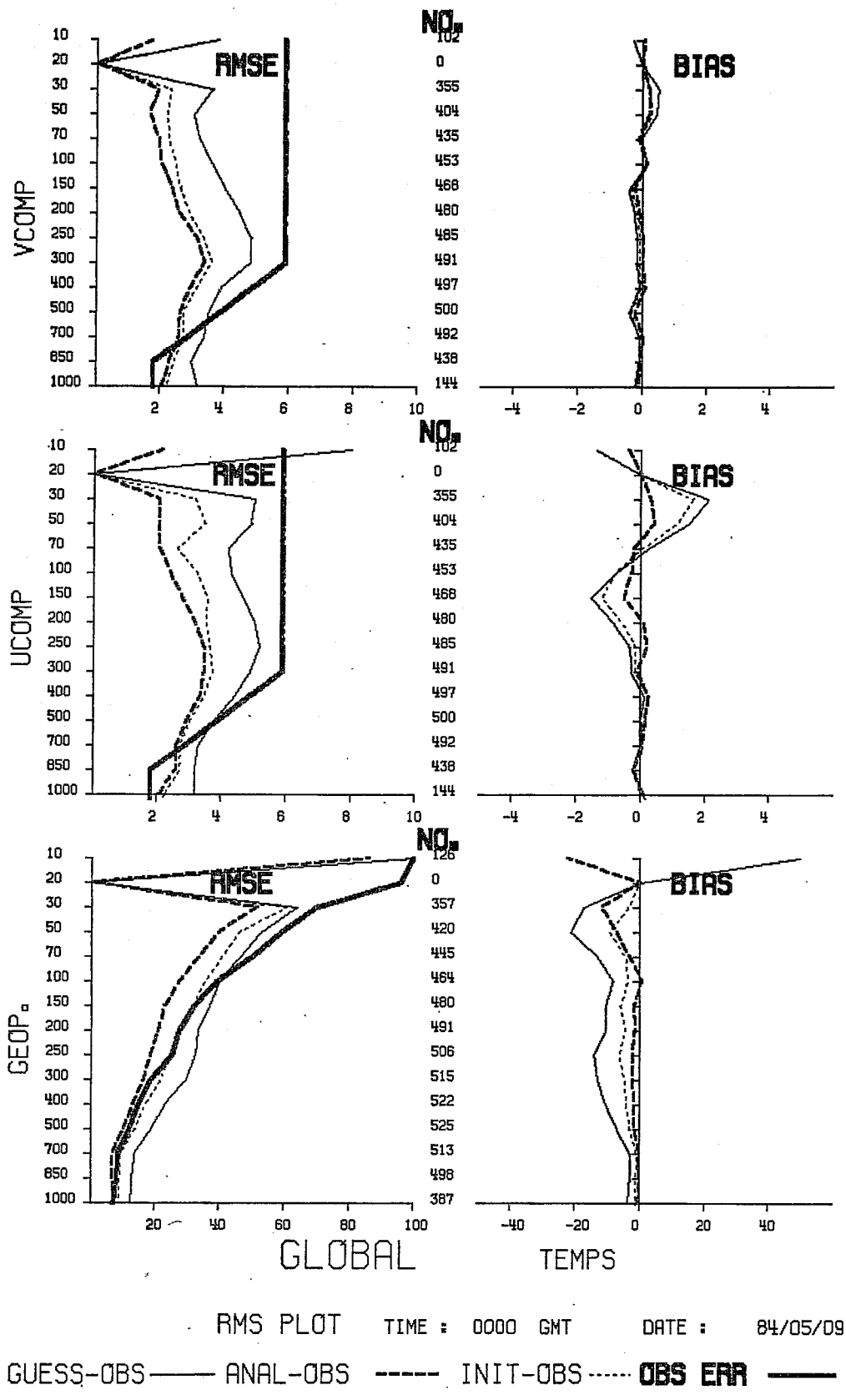

Fig. 19a Old system. Fit of TEMP observations to the assimilation fields for 00Z 9.5.84. Vertical scale is pressure in mb. The horizontal scale has units of m. (for geopotential) and m sec^{-1} (for wind components u and v). The ascribed observation error (bold continuous line) is that used in the old system.

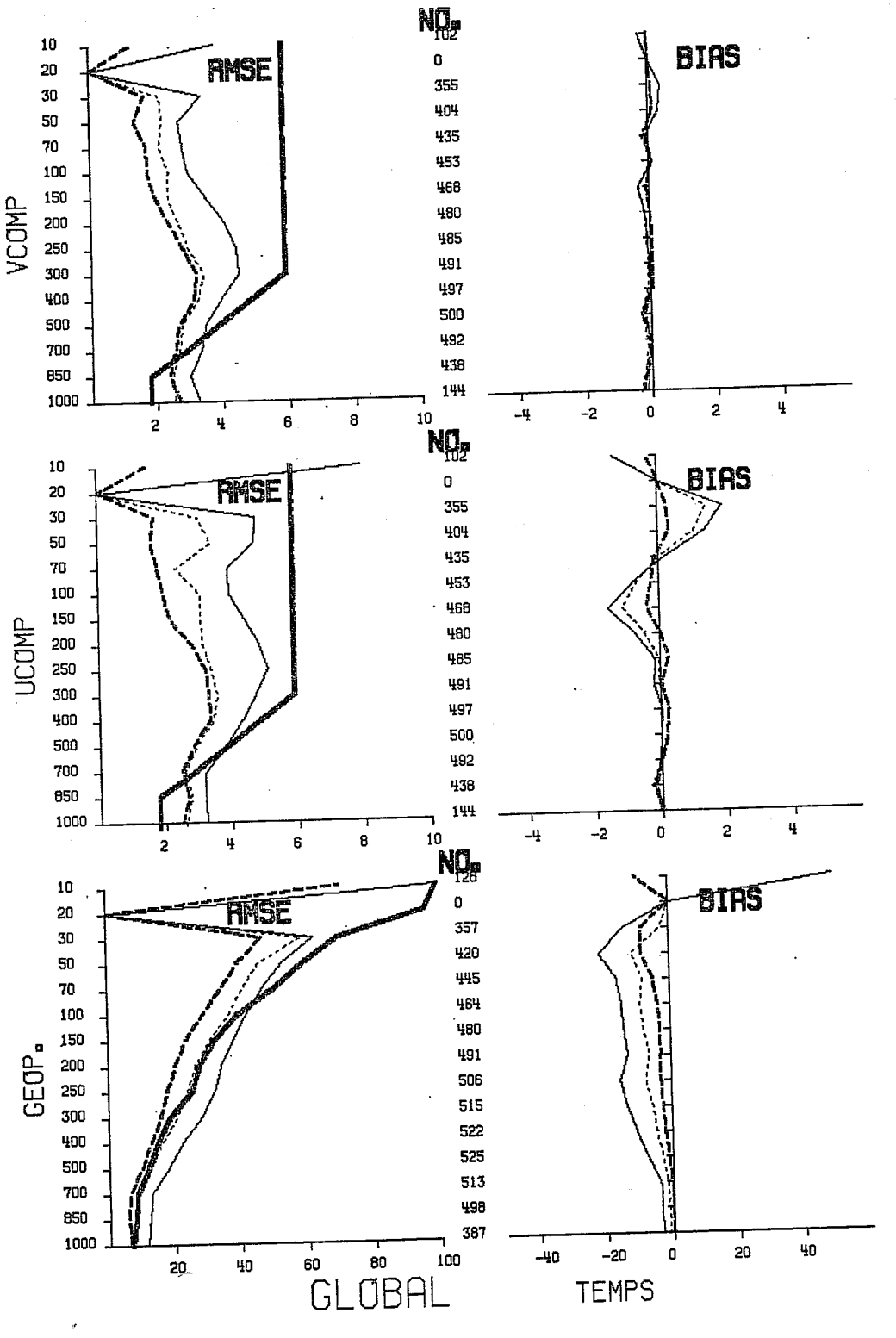

Fig. 19b As for Fig. 19a, but for the new system.

6.2 Fit to the observations

A basic measure of an analysis is its ability to fit the observational data it uses with appropriate accuracy. Fig.19(a) and (b) shows the fit of first guess, analysed and initialised fields to the global network of TEMP stations, for a datum time selected at random from the 30 days available. The observation data set used in the diagram, common to both the old and the new system, is the data which was accepted and used by the new system. This of course could be interpreted as giving an advantage to the new system in the subsequent evaluation. Some screening of the observational data is necessary, to exclude gross errors that would otherwise invalidate the statistics, and, as already discussed, the data set used by the new system is judged to be better in terms of quality control screening. Evaluations of both old and new systems have been made using the data selected by their respective quality control judgements; because the old system frequently accepted incorrect data, the old system was found to fit its selection of data less well than it fits the new system's selection of data. In this sense then, the intercomparison is sympathetic to the new system.

Comparing the fit to data, the geopotential fit of the new system is slightly better, in the rms sense, than it was previously for all three elements of the assimilation - first guess, analysis and initialisation. The bias is worse in the new system in the upper troposphere. A substantial part of this bias in the upper troposphere may stem from instrumental biases in the observations. However the new system has reduced the ascribed error of the first guess field and any systematic deficiency in the model may therefore become more evident; one such deficiency may be a small systematic cooling of the model in the early part of its predictions. The partitioning of the bias into instrumental and model components is currently the subject of investigation. A point to be borne in mind is that this evaluation against observations, while being global in the sense that all accepted TEMP data is being used, is obviously biased towards these regions where such data are plentiful, in particular the extratropical land areas of the Northern Hemisphere.

The u and v components of the wind fitting both show appreciable benefits fr the new system in the upper troposphere, for the three elements of the assimilation, in the rms sense. The wind biases for the two system are very similar and generally very small.

Given that these results are heavily influenced by the data dense regions where there is relatively modest scope for improving the analysis, Fig.19 is an understatement of the true gain. Corresponding plots (not shown) are available for the tropical belt and for the Southern Hemisphere; these show the same type of change as the global picture, but with the improvements in the fitting of the wind data being very pronounced - the initialised fields the new system showing a similar fit to the data as do the analysed fields o the old system.

The overall impression of the analyses is that the new system fits the observations at least as well as, and generally better than, the old system, with the single exception of the overall bias in the fit of TEMP geopotentials. A final point regarding the geopotential bias is that it now appears to have a more regular vertical structure, which may make the proble more amenable to a corrective treatment as the result of further investigation.

6.3 The relative roles of F, A, I

A good appreciation of the working of the assimilation scheme can be gained examining the relative roles of the prediction model, the analysis and the initialisation, as discussed by Hollingsworth and Arpe (1982). These three components between them approximate the evolution of the true atmosphere state. Representing the rms changes due to Forecast, Analysis and Initialisation as F, A, and I respectively, a desirable state is one in whi F>A>I (having first satisfied ourselves that the analysis draws well to the correct observations). As discussed by Shaw (1983), a clear distinction between northern and southern hemisphere regimes has existed in the operational assimilations up to the present time. In the northern hemisphe F>A>I - most of the evolution is indeed captured by the model, with the analysis making relatively modest adjustments to a fairly accurate first guess, and the initialisation making yet more modest adjustments to the

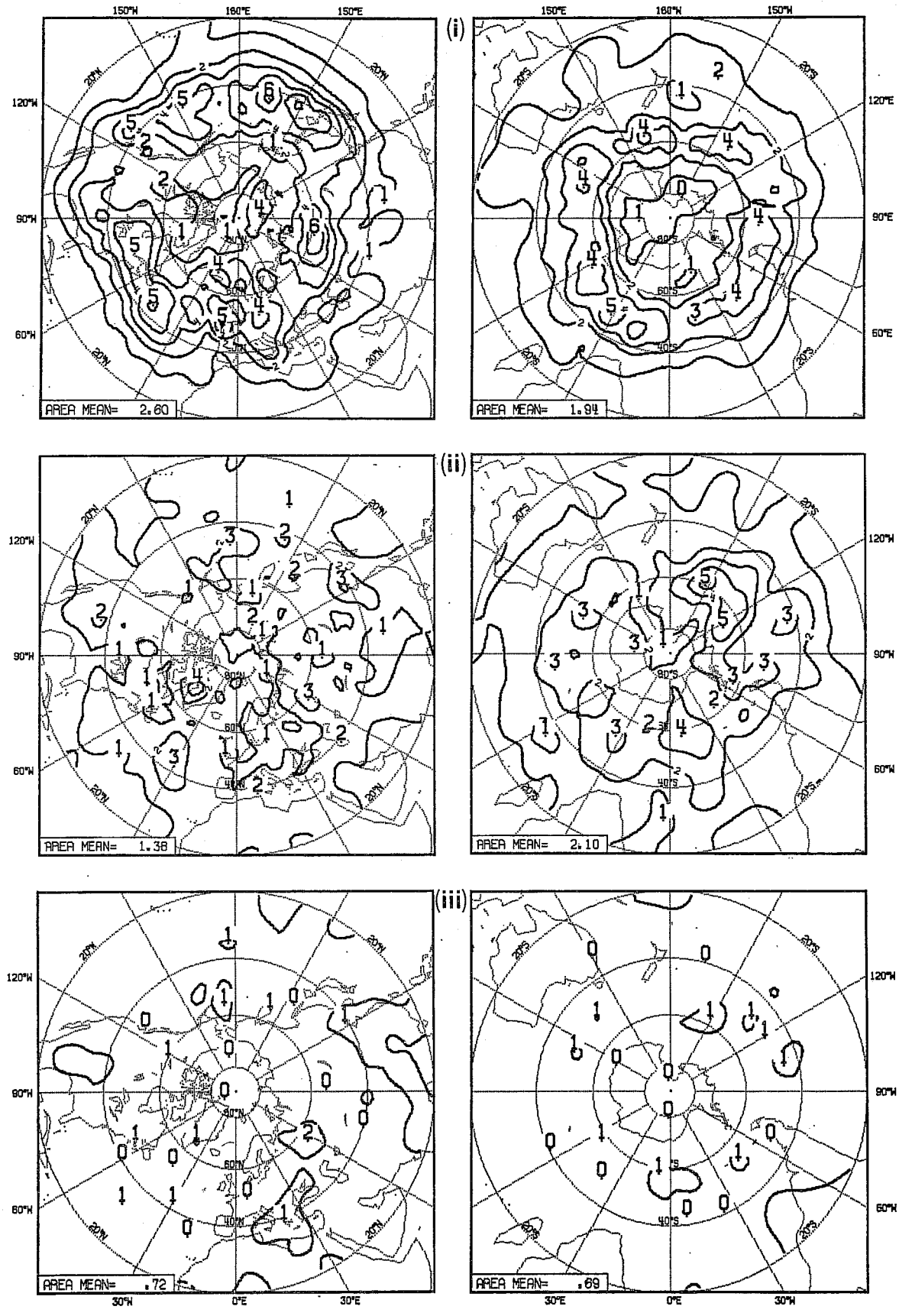

Fig. 20a RMS changes in geopotential (in dams) brought about by (i) 6hr forecast (ii) analysis (iii) initialisation, based on 16 successive mainhour (00 and 12GMT) assimilations 26.11.83-4.12.83, using the old system.

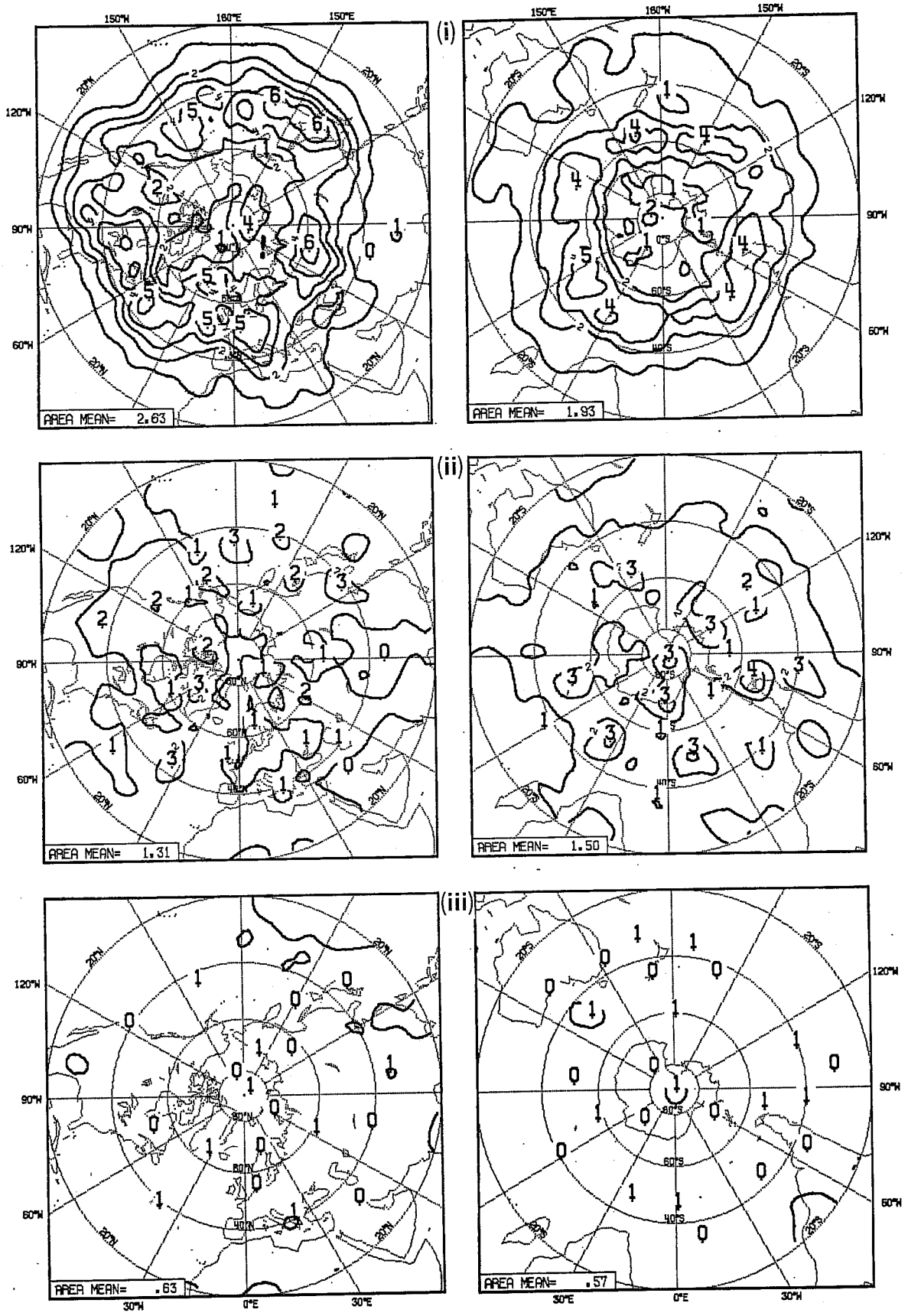

Fig. 20b As for Fig. 20a, but using the new system.

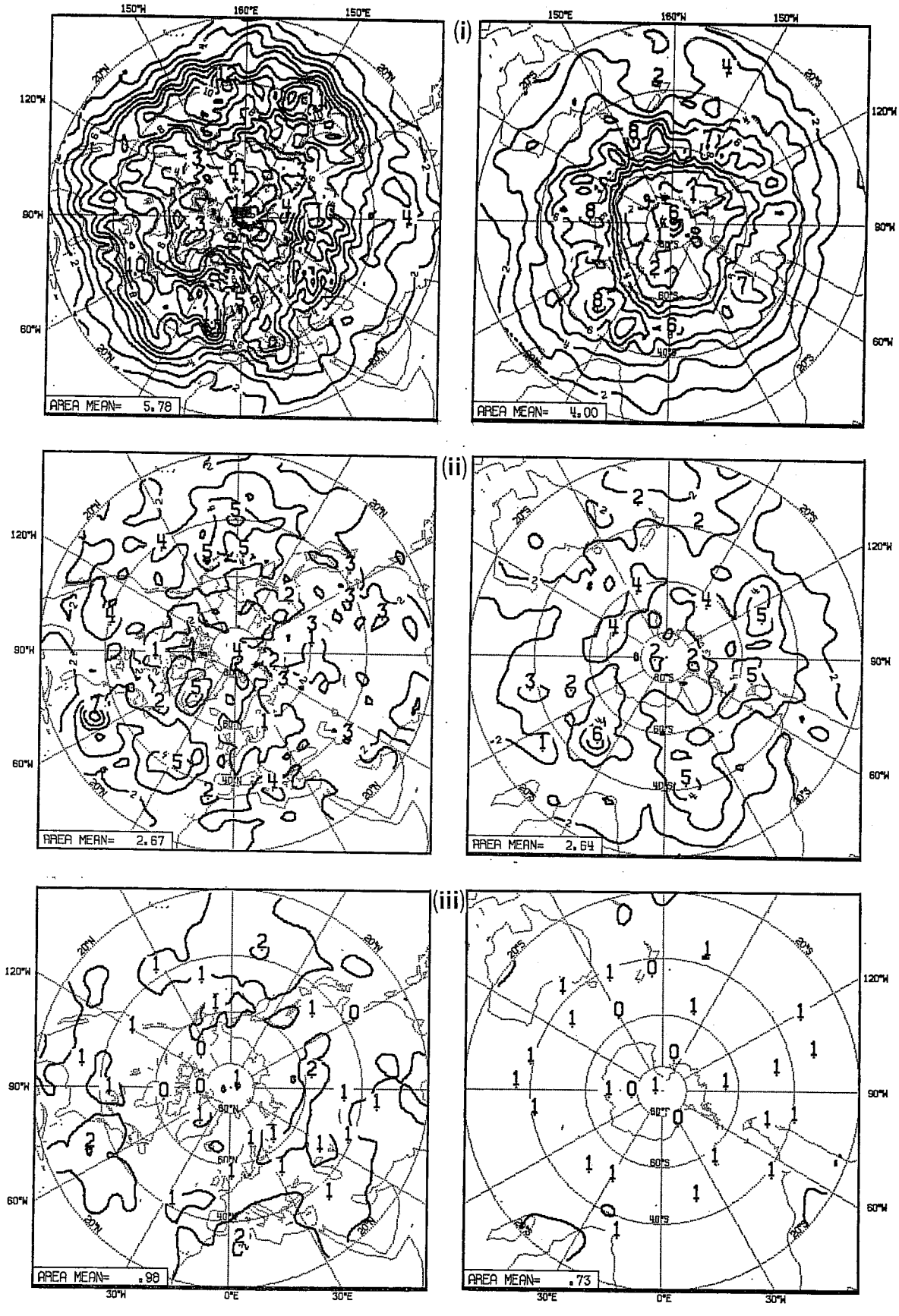

Fig. 21a As for Fig. 20a, for vector wind (in m sec^{-1}).

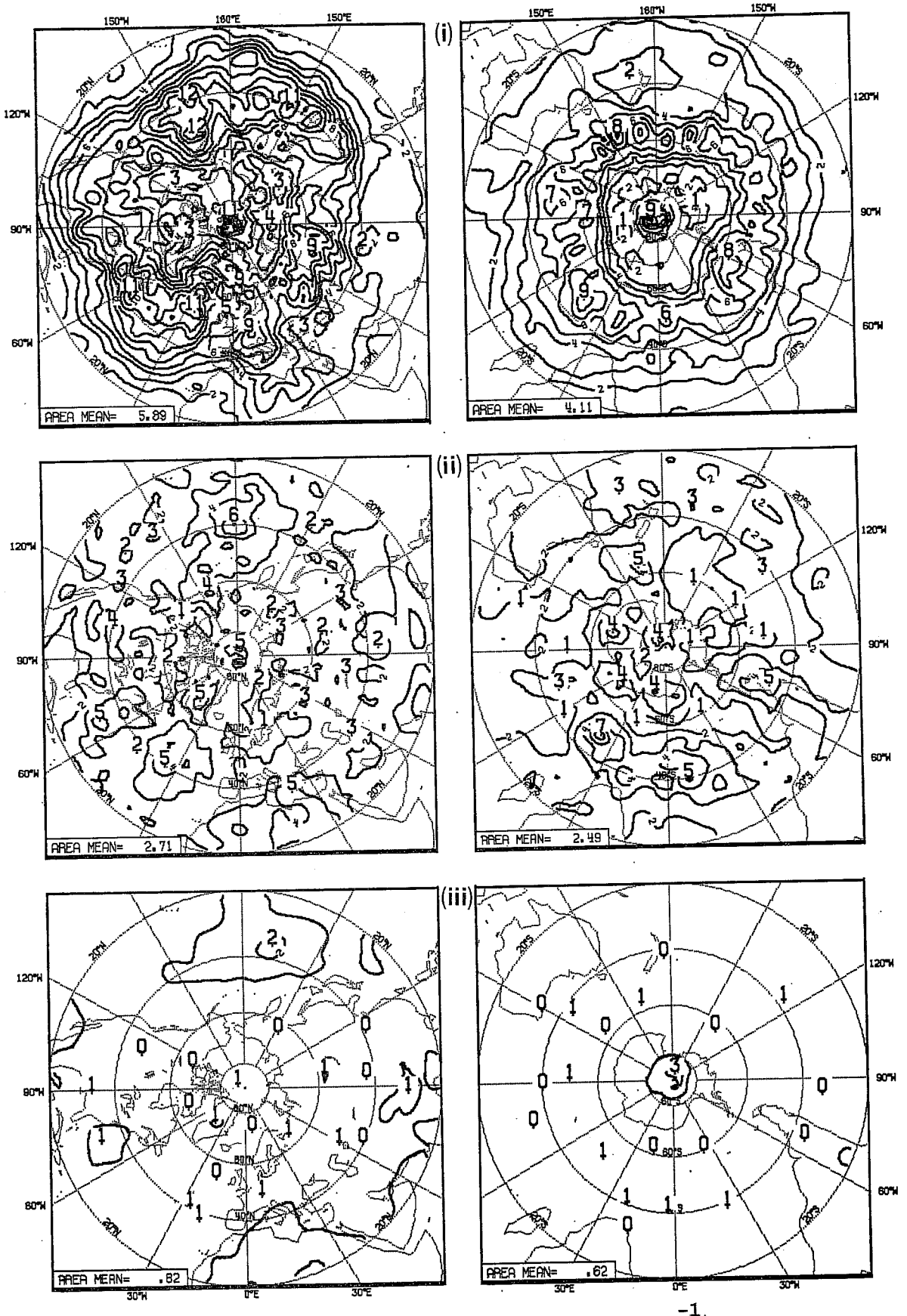

Fig. 21b As for Fig. 20b, for vector wind (in m sec^{-1}).

analysis. However in the southern hemisphere, the relationship to date has been A>F>I - the forecast model making appreciable changes in a typical 6 h evolution, but the analysis then makes swinging adjustments to this first guess field.

The relative roles of the three components have been evaluated for both the old and the new analysis systems, based on the composite of 16 main hour (00 and 12 GMT) evaluations for the period 26 Nov-4 Dec 1983. The quantities computed are the rms changes in geopotential and vector wind at 500 mbn, for the three components; the results are shown in Figs.20 (geopotential) and 21 (wind).

Looking first at the 6 hr forecast changes in the northern hemisphere, the old and new systems show similar, but not identical patterns. The model is most active in the mid latitude depression belt, as one would expect. The new system suggests that the model has become a little more active as a consequence of the analysis changes (the area mean changes have increased from 2.60 to 2.63 dam and from 5.78 to 5.89 m/s for geopotential and wind respectively). This may be a consequence of the better delineation of baroclinic zones in the new analyses, though the changes are only modest. The analysis changes for the northern hemisphere are also similar for the old and new system. The geopotential changes in the new system are more modest (1.31 c/f 1.38 m) while the wind changes are enhanced (2.71 m sec^{-1} c/f 2.67 m sec^{-1}). This is consistent with one of the results discussed earlier - the new analysis draws much more closely now to the wind observations, producing slightly bigger wind increments despite the fact that the first guess wind field is more accurate than previously. A further point to note is that the analysed changes in the old system contain appreciable contributions arising from the acceptance of incorrect data, which will produce typically large analysis changes. Where such errors are persistent they will show up as localised maxima on the analysis components of Figs. 20 and 21, and such a feature is suggested in the localised maximum in the analysis component for wind in the old system at approximately 33°N 66°W. A very encouraging indication that the new system provides a better analysis than the old is found in the initialisation changes of both geopotential and wind, where the new system produces appreciable smaller changes. Expressed as rms changes

the reductions are approximately 12-15%; as variances, the reductions are approximately 30-35%. It suggests that the analysed geopotential and wind increments are now more coherent and balanced than was previously the case.

Turning to the southern hemisphere, similarly encouraging improvements are seen in the reduction of the initialisation changes. The forecast evolution components of the old and new system are similar and unremarkable. What has changed, quite dramatically, is the magnitude of the analyses changes in the new system. In terms of area means, these are reduced from 2.10 to 1.50 dam (geopotential) and from 2.64 to 2.49 m sec^{-1} (wind). The analysis changes are substantially smaller than the forecast changes, for the new system. It is considered that the biggest single cause of this change in the character of the southern hemisphere assimilations has been the decision to reduce the role of the PAOB data. It is particularly noticeable that the analysis changes in the south east Pacific and south Atlantic are reduced in the new system; these are areas where perhaps the PAOBs are least accurate. In both the new and old systems, localised maxima are evident in the analysis changes (e.g. at approximately 48°S, 40°E, particularly in the wind components). These may be indicative of unresolved data problems, or they may be localised indications of larger scale errors in the predictive model.

6.4 The quality of the forecasts

Having produced a revised analysis system capable of improving the analysed state in terms of improved fit to data, better discrimination of good and bad data and smaller initialisation changes, it remains to demonstrate that these revised analyses yield better forecasts. From the original experiments for May and Nov/Dec 1983, a total of twelve 10-day forecasts have been run and compared with the operational forecasts. Sensitivity to the analysis changes are clearly seen in the forecasts on the time scales of interest to ECMWF, namely 4-10 days. Comparing new with old, some forecasts were better, some were worse.

The standard means of evaluating a forecast at ECMWF is to examine the correlation of the anomaly (from climatology) of the predicted state and of the verifying analysed state. Such an example is shown in Fig. 22, for the extratropical northern hemisphere troposphere, for two forecasts from 12 GMT 6 May 1983. The forecasts are based on the old operational analysis and an analysis produced using the new analysis system, as indicated. The limit of

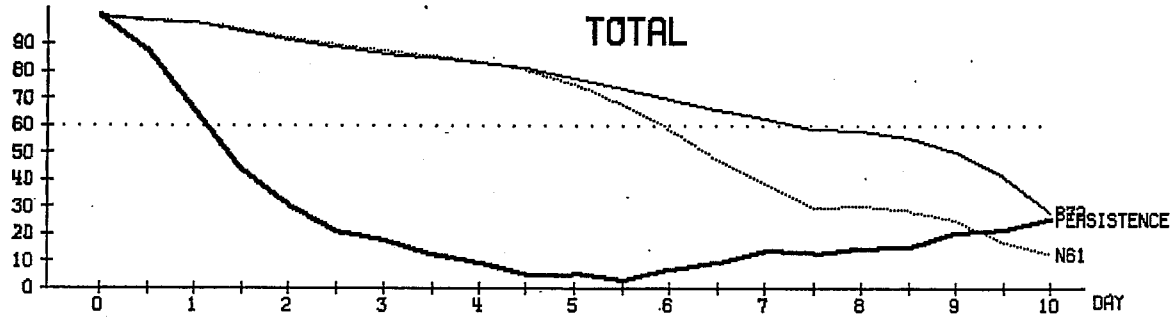

Fig. 22 Anomaly (from climatology) correlation scores measured against days of prediction for forecasts from 12GMT 6.5.83, for the northern hemisphere extra tropical (20°N - 82.5°N) troposphere (1000-200 mb). The continuous line is for the new analysis system ; the dotted line is for the old analysis system, and the bold continuous line is a persistence forecast. The horizontal line of dots mask the 60 % correlation threshold.

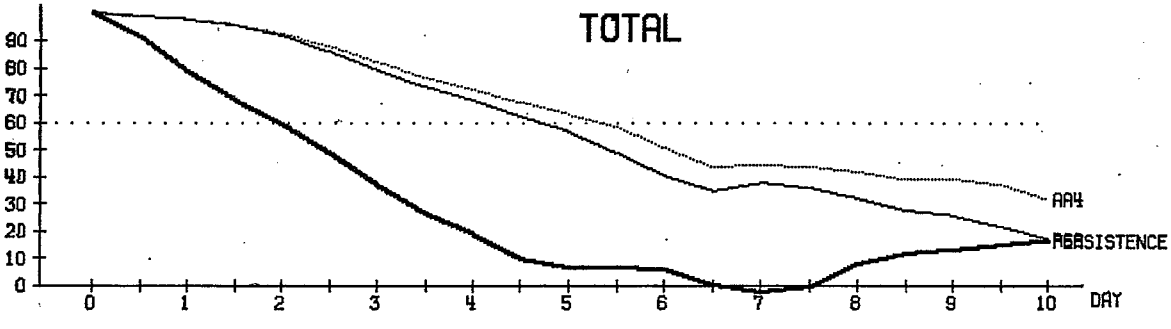

Fig. 23 As Fig. 22, for 12Z 4.12.83.

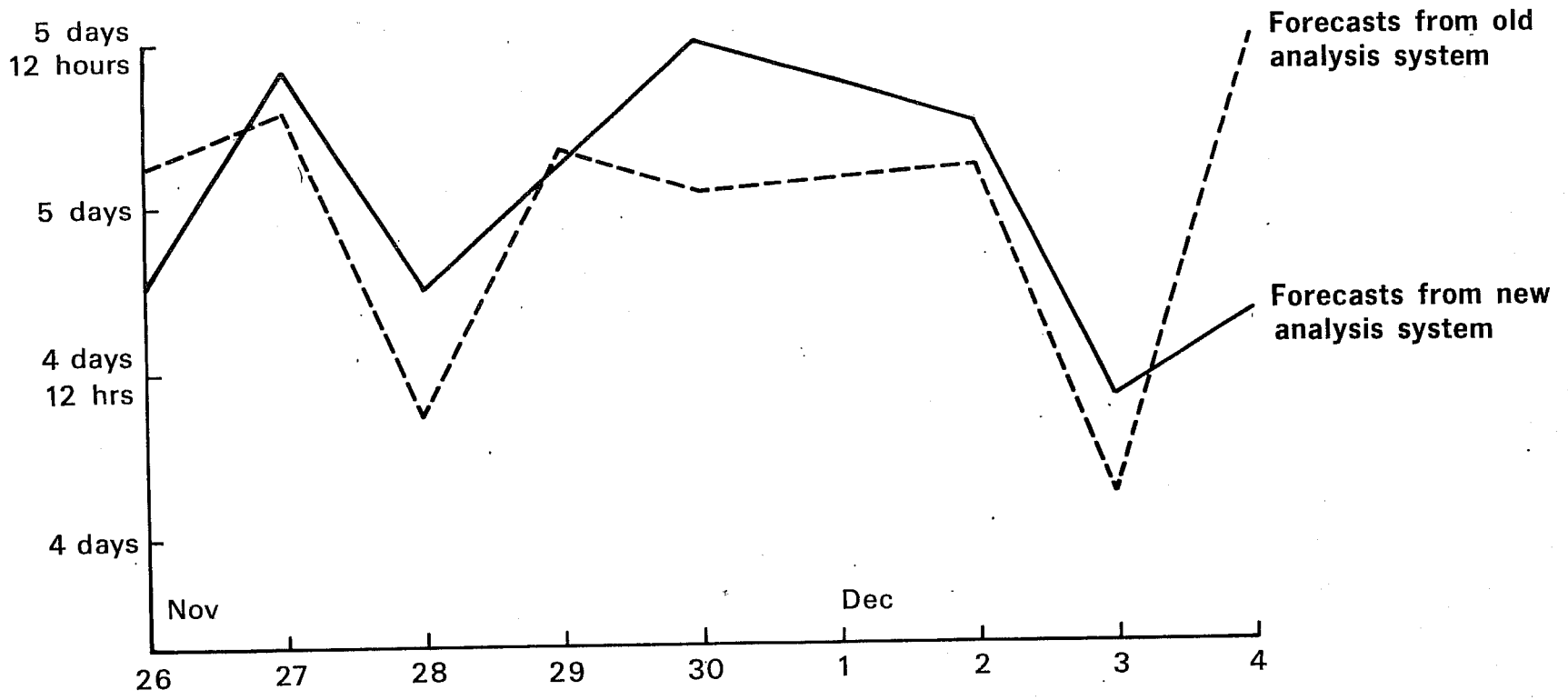

Fig. 24 Time in forecast at which 60% anomaly threshold is reached for forecasts run from successive days (12GMT start time) for 26.11.83-4.12.83

predictive skill is usually judged to be reached when the anomaly correlation falls between 0.6, as indicated by the horizontal dotted line in Fig. 22. The new system is seen to produce an improvement in the limit of predictability of approximately 30 hrs. Fig. 23 shows another case, from 12Z 4.12.83, where the new system produces a degradation of 15 hrs compared to the operational forecast.

Gain in predictability in hours based on NH anomaly correlations

6/5	8/5	10/5	26/11	27/11	28/11	29/11	30/11	1/12	2/12	3/12	4/12
+30	+9	-7	-11	-3	+9	-1	+11	+2	+3	+7	-15

Average = +2.8

The above table summarises the gains in predictive skill for the 12 cases. The two examples referred to above are the extremes of the sample. Based on the 12 cases an average improvement of 2.8 hrs is found; however this sample is very small and exclusion of individual cases produces a quite different impression. That some of the medium range forecasts are worse is, of course, worrying. The 6 hr forecasts are known to be better, at least in the rms sense, in their fit to verifying observations. Indeed detailed investigation of the forecasts for 12Z 26 Nov.83, when the new system performed badly, suggests that the new analysis system produced a better analysis in the critical areas from where the errors in the forecast are seen to grow. No convincing explanation of the two most seriously degraded forecasts (26 Nov and 4 Dec) has been found.

A reassuring signal in the November sequence of forecasts is in the consistency of forecasts from successive days. Fig. 24 is a plot of the time in the forecast when the 6 anomaly correlation is reached, for forecasts made on successive days, for the new and old analysis systems. The new thresholds are seen to be generally advanced in time compared to the old, as suggested by the above table. In addition, there is less variability in the quality of forecasts with the new system. This is perhaps to be expected in the sense that the improved quality control measures of the new system eliminate many of the random errors present in the initial states arising in the old system.

Fig. 25 shows the results corresponding to Fig. 22, for the Southern Hemisphere. The verifying analysis is the old operational analysis, and it is clear from the difference in the initial states, and its temporal persistence, that assessment of the forecasts are now very dependent on the verifying analyses, at least in the first three days of the forecst. The same is true for the tropical region. Based on the foregoing assessment of the analyses, it is considered better to verify against the revised analyses.

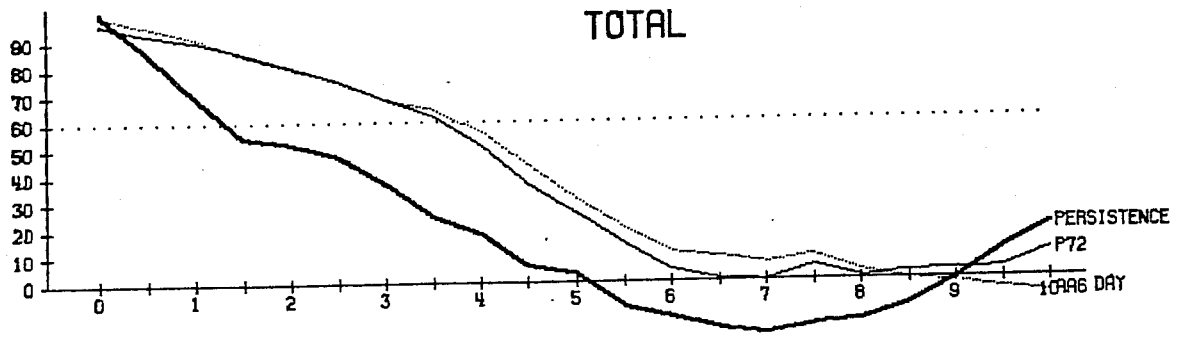

Fig. 25 As Fig. 22 but for the southern hemisphere.

The table below shows such evaluations for the tropics for the May 1984 sequence of cases; missing values indicate that the forecasts are unavailable. The 24 hr forecasts are invariably better, with the D+2 day forecasts (at the limit of our tropical predictive skill) showing some gains and some losses.

Tropical scores - 200 mb rms vector wind error

	T + 24		T + 48	
	Old	New	Old	New
7 May	6.6	5.9	-	-
10 May	7.2	6.8	8.6	8.8
11 May	7.0	6.3	-	-
12 May	6.5	6.1	7.4	7.6
13 May	6.5	6.0	8.2	8.2
14 May	7.0	6.5	8.6	8.5
15 May	6.6	5.6	-	-
16 May	6.4	6.2	8.6	9.0
17 May	7.5	6.6	9.0	9.0
18 May	7.2	6.4	-	-
Average	6.85	6.27		

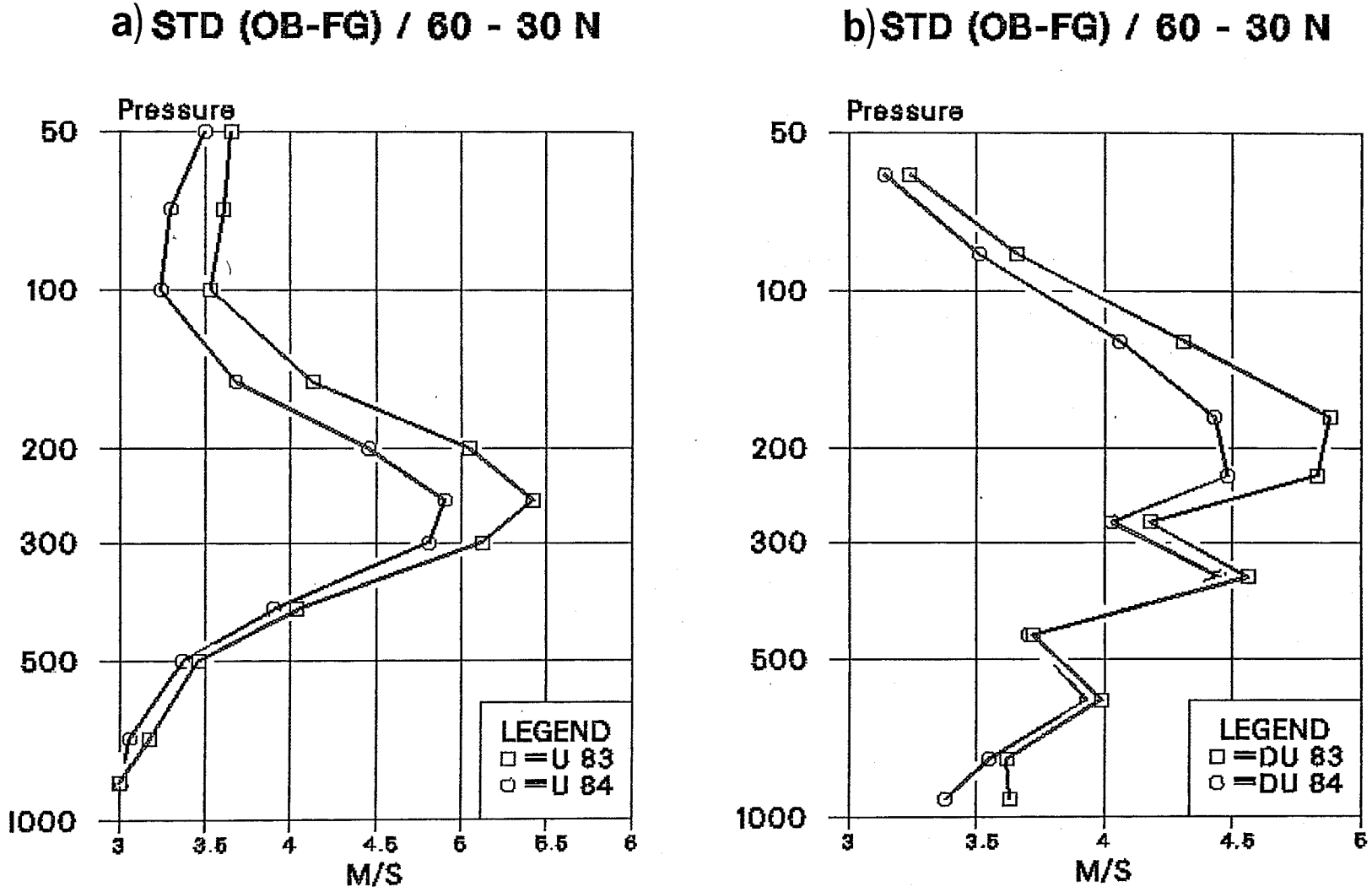

Fig. 26 Standard deviation of difference between observation and six hour forecast for a) U and b) ΔU for summers (June-August) 1983 and 1984 in northern mid-latitudes (60°-30°N). Units: m/s.

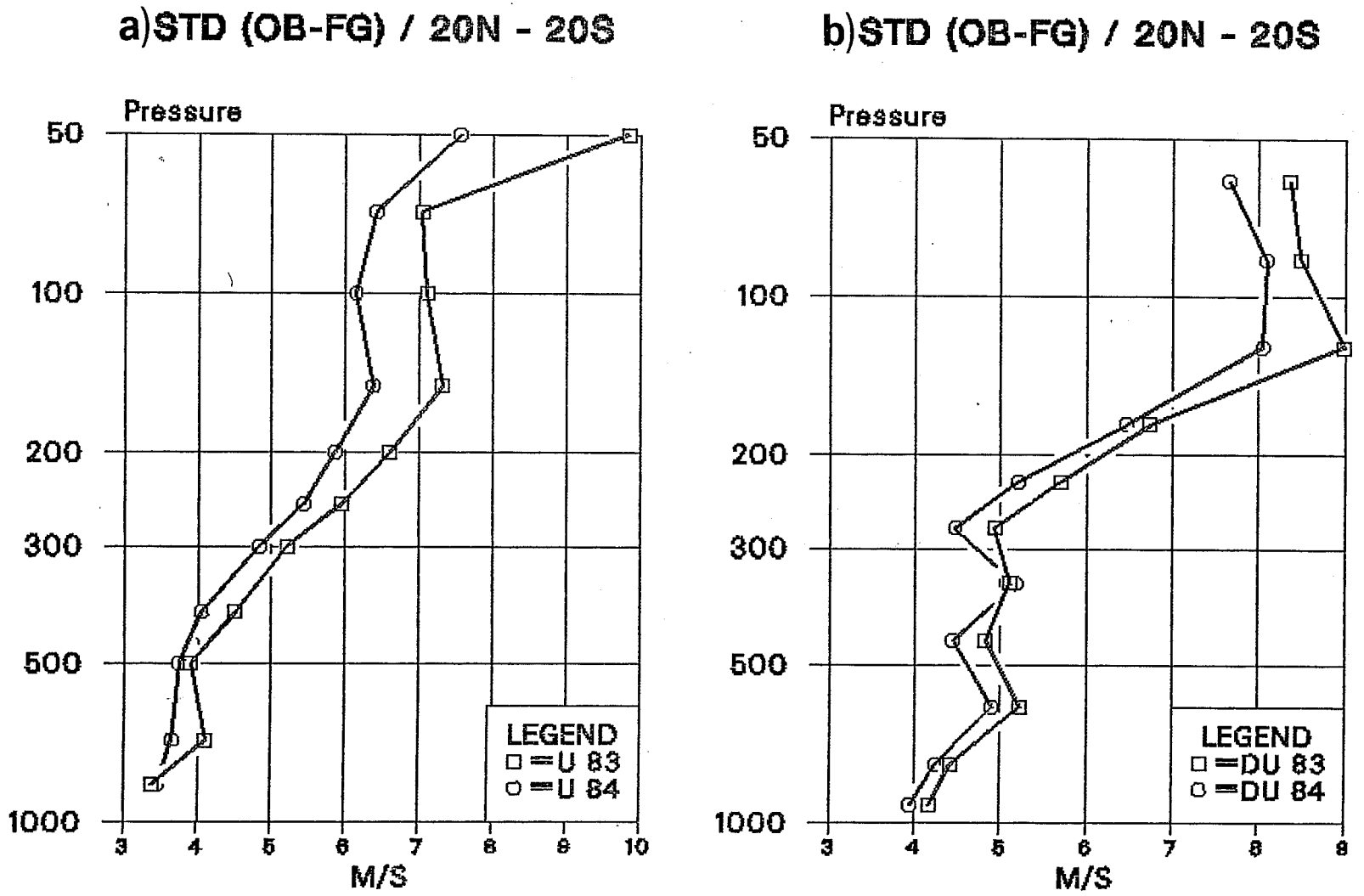

Fig. 27 As for Fig. 26, but for the tropics (20^{o}-20^{o}S).

7. CONCLUSIONS

It is concluded that substantial gains have been made in the quality of the analyses as a result of the modifications described in the opening sections of the paper. The set of modifications represent the first comprehensive revision of the ECMWF analysis scheme. Many further revisions are possible; some of these, particularly relating to data selection, and more generalised formulations of the OI relationships, cannot be accommodated within the framework of the existing software and so will await a re-write of the system, which is currently in hand.

The quality of the analyses can be estimated from the accuracy of the subsequent six hour forecasts as measured against observtions. A considerable reduction of the perceived forecast error has been achieved during the past year. Fig. 26 compares the standard deviation of (observed - first guess) in summers (June-August) 1983 and 1984 for (a) the zonal wind component and (b) its vertical shear in northern midlatitudes. Improvements of about 0.5 ms^{-1} are found at and above jet level for the predicted zonal wind, and a smaller but consistent reduction of errors in forecasted wind shear. The gains in the tropical belt are more striking - between 0.5 and 1 ms^{-1} for the zonal wind (Fig. 27a). The accuracy of the predicted wind shear is consistently higher in summer 1984 than in the previous summer (Fig. 27b). In addition to the analysis revisions, the diurnal cycle has been introduced during the past year.

The progress made, and the realisation that most aspects of the analysis can be improved further, are both encouraging for future studies of assimilation techniques at the Centre.

REFERENCES

Daley, R., 1983: Spectral characteristics of the ECMWF objective analysis system. ECMWF Tech.Rep.No.40, 119pp.

ECMWF Staff Members 1984: Monitoring of observation quality by a data assimilation system. To be submitted.

Hollingsworth, A. and Arpe, K., 1982: Biases in the ECMWF data assimilation system. ECMWF Tech.Memo.No.46.

Hollingsworth, A. and Lönnberg, P. 1984: The statistical structure of short-range forecast errors. To be submitted.

Lönnberg, P., and Shaw, D. (Eds), 1983: ECMWF Data Assimilation Scientific Documentation.

Lorenc, A.C., 1981: A global three-dimensional multivariate statistical interpolation scheme. Mon.Wea.Rev., 109, 701-721.

Louis, J.-F., (Ed), 1983: ECMWF Forecast Model: Physical Parameterisation.

Shaw, D., 1983: Performance of the Centre's Data Assimilation Scheme. ECMWF/SAC(83)9.

TROPICAL H CORRELATIONS(*1000) & ERRORS(M/S)

	1000	850	700	500	400	300	250	200	150	100	70	50	30	20	10
1000	1000	560	142	-37	-51	-56	-170	-170	-161	-47	25	56	78	86	93
850	560	1000	485	228	159	95	57	19	0	104	136	143	146	146	146
700	142	485	1000	656	593	494	428	361	342	352	274	225	185	169	155
500	-37	228	656	1000	881	751	665	599	551	504	359	276	211	184	161
400	-51	159	593	881	1000	914	818	748	692	578	381	272	189	155	126
300	-56	95	494	751	914	1000	855	789	732	580	362	244	156	120	89
250	-170	57	428	665	818	855	1000	865	798	618	376	246	149	110	77
200	-170	19	361	599	748	789	865	1000	846	608	338	198	161	123	95
150	-161	0	342	551	692	732	798	846	1000	665	570	475	380	285	190
100	-47	104	352	504	578	580	618	608	665	1000	665	570	475	380	285
70	25	136	274	359	381	362	376	338	570	665	1000	665	570	475	380
50	56	143	225	276	272	244	246	198	475	570	665	1000	665	570	475
30	78	146	185	211	189	156	149	161	380	475	570	665	1000	665	570
20	86	146	169	184	155	120	110	123	285	380	475	570	665	1000	665
10	93	146	155	161	126	89	77	95	190	285	380	475	570	665	1000
	3.2	5.1	5.2	5.4	6.1	7.4	9.5	10.5	10.2	9.3	11.5	13.6	16.0	17.3	18.6

Table 1a. Vertical forecast error correlations (*1000), together with the variances at the levels (1000,..., 10mb). The variances are considered to be representative of continental areas. Tropical winds in old system. Units m s^{-1}.

TROPICAL U CORRELATIONS(*1000) & ERRORS(M/S)

	1000	850	700	500	400	300	250	200	150	100	70	50	30	20	10
1000	1000	433	112	8	2	0	0	0	0	0	0	0	0	0	0
850	433	1000	542	84	22	4	1	0	0	0	0	0	0	0	0
700	112	542	1000	352	126	34	9	3	0	0	0	0	0	0	0
500	8	84	352	1000	681	305	122	46	4	0	0	0	0	0	0
400	2	22	126	681	1000	671	344	156	18	0	0	0	0	0	0
300	0	4	34	305	671	1000	735	423	74	1	0	0	0	0	0
250	0	1	9	122	344	735	1000	771	202	4	0	0	0	0	0
200	0	0	3	46	156	423	771	1000	424	16	0	0	0	0	0
150	0	0	0	4	18	74	202	424	1000	139	5	0	0	0	0
100	0	0	0	0	0	1	4	16	139	1000	213	34	8	2	0
70	0	0	0	0	0	0	0	0	5	213	1000	475	190	66	19
50	0	0	0	0	0	0	0	0	0	34	475	1000	687	347	138
30	0	0	0	0	0	0	0	0	0	8	190	687	1000	723	374
20	0	0	0	0	0	0	0	0	0	2	66	347	723	1000	723
10	0	0	0	0	0	0	0	0	0	0	19	138	374	723	1000
	1.0	1.3	2.2	2.9	3.8	5.8	5.0	5.3	5.5	5.0	4.0	4.0	4.7	4.7	4.7

Table 1b. Same as 1a, but for revised analysis system.

Inst. Type	1000	850	700	500	400	300	250	200	150	100	70	50	30	20	10
SONDE/PILOT WIND	1.8	1.8	2.9	3.4	3.9	4.9	5.5	5.9	5.9	5.9	5.9	5.9	5.9	5.9	5.9
SONDE GEOP.	7.0	8.0	8.6	12.1	14.9	18.8	25.4	27.7	32.4	39.4	50.3	59.3	69.8	96.0	114.2
SONDE THICKNESS	-	5.4	6.3	12.9	9.8	13.5	9.6	13.1	17.7	24.9	24.0	26.6	47.0	45.1	91.4
SATEMS															
Clear path	-	12.0	10.6	15.8	11.8	16.9	9.1	11.1	14.3	20.2	17.8	17.7	28.4	23.8	40.6
Partly cloudy	-	12.0	11.7	15.8	12.4	17.7	10.1	12.4	14.3	20.2	17.8	17.7	28.4	23.8	40.6
Microwave	-	12.0	12.3	15.8	13.7	19.4	10.1	12.4	14.3	20.2	17.8	17.7	28.4	23.8	40.6
SATOBS															
GOES	4.2	4.2	5.1	5.9	6.7	7.5	7.5	7.5	7.5	7.5	7.5	7.5	7.5	7.5	7.5
METEOSAT	7.2	7.2	7.5	7.8	8.1	8.4	8.4	8.4	8.4	8.4	8.4	8.4	8.4	8.4	8.4
HIMAWARI	6.1	6.1	7.9	9.7	11.5	13.3	13.3	13.3	13.3	13.3	13.3	13.3	13.3	13.3	13.3
AIDS/ASDAR	1.8	1.8	2.9	3.9	4.9	5.9	5.9	5.9	5.9	5.9	5.9	5.9	5.9	5.9	5.9
AIREP	7.2	7.2	7.5	7.8	8.1	8.4	8.4	8.4	8.4	8.4	8.4	8.4	8.4	8.4	8.4
PAOBS	14.0														
SYNOP/SHIP WIND	3.6														
SYNOP/SHIP GEOP.	7.0														
DRIBU GEOP.	14.0														

Table 2.(a) Rms observation errors. Units $msec^{-1}$ and m

Inst. Type	1000	850	700	500	400	300	250	200	150	100	70	50	30	20	10
SONDE/PILOT WIND	2.2	2.5	2.6	3.1	3.7	3.8	3.3	3.0	2.8	2.4	2.4	2.4	2.5	3.1	3.5
SONDE GEOP.	5.0	5.4	6.0	9.4	11.6	13.8	14.2	15.2	18.2	21.4	25.2	29.8	31.2	38.1	50.0
SONDE THICKNESS	-	5.4	6.3	12.9	9.8	13.5	9.6	13.1	17.7	24.9	24.0	26.6	47.0	45.1	91.4
SATEMS															
Clear path	-	12.0	10.6	15.8	11.8	16.9	9.1	11.1	14.3	20.2	17.8	17.7	28.4	23.8	40.6
Partly cloudy	-	12.0	11.7	15.8	12.4	17.7	10.1	12.4	14.3	20.2	17.8	17.7	28.4	23.8	40.6
Microwave	-	12.0	12.3	15.8	13.7	19.4	10.1	12.4	14.3	20.2	17.8	17.7	28.4	23.8	40.6
SATOBS															
GOES															
METEOSAT	2.5	2.5	2.5	2.5	5.0	5.0	5.0	5.0	5.0	5.0	5.0	5.0	5.0	5.0	5.0
HIMAWARI															